

University of Montana

ScholarWorks at University of Montana

Graduate Student Theses, Dissertations, &
Professional Papers

Graduate School

1981

Alteration petrology and mineralization of the Flathead Mine Hog Heaven Mining District Montana

C. Carey Cossaboom
The University of Montana

Follow this and additional works at: <https://scholarworks.umt.edu/etd>

Let us know how access to this document benefits you.

Recommended Citation

Cossaboom, C. Carey, "Alteration petrology and mineralization of the Flathead Mine Hog Heaven Mining District Montana" (1981). *Graduate Student Theses, Dissertations, & Professional Papers*. 7602.
<https://scholarworks.umt.edu/etd/7602>

This Thesis is brought to you for free and open access by the Graduate School at ScholarWorks at University of Montana. It has been accepted for inclusion in Graduate Student Theses, Dissertations, & Professional Papers by an authorized administrator of ScholarWorks at University of Montana. For more information, please contact scholarworks@mso.umt.edu.

COPYRIGHT ACT OF 1976

THIS IS AN UNPUBLISHED MANUSCRIPT IN WHICH COPYRIGHT SUBSISTS. ANY FURTHER REPRINTING OF ITS CONTENTS MUST BE APPROVED BY THE AUTHOR.

MANSFIELD LIBRARY
UNIVERSITY OF MONTANA
DATE: 1981

ALTERATION PETROLOGY AND MINERALIZATION
OF THE FLATHEAD MINE,
HOG HEAVEN MINING DISTRICT,
MONTANA

by

C. Carey Cossaboom

B.S., Florida State University, 1976

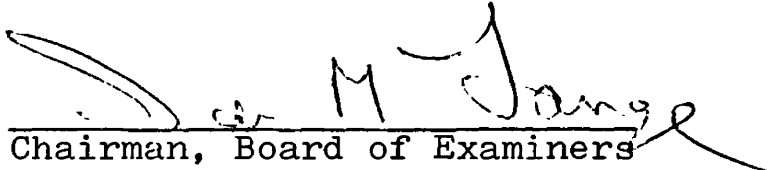
Presented in partial fulfillment of the
requirements for the degree of

Master of Science

UNIVERSITY OF MONTANA

1981

Approved by:


Chairman, Board of Examiners


Dean, Graduate School

September 17, 1981
Date

UMI Number: EP38403

All rights reserved

INFORMATION TO ALL USERS

The quality of this reproduction is dependent upon the quality of the copy submitted.

In the unlikely event that the author did not send a complete manuscript and there are missing pages, these will be noted. Also, if material had to be removed, a note will indicate the deletion.



UMI EP38403

Published by ProQuest LLC (2013). Copyright in the Dissertation held by the Author.

Microform Edition © ProQuest LLC.

All rights reserved. This work is protected against unauthorized copying under Title 17, United States Code



ProQuest LLC.
789 East Eisenhower Parkway
P.O. Box 1346
Ann Arbor, MI 48106 - 1346

ABSTRACT

Cossaboom, C. Carey, M.S., Fall, 1981

Alteration Petrology and Mineralization of the Flathead Mine, Hog Heaven Mining District, Montana (104 pp.)

Director: Ian M. Lange 

The Flathead mine is an epithermal silver-lead deposit hosted by Tertiary volcanic rocks; gold, copper, and zinc values are less important. The characteristics of the alteration and mineralization in the low-grade fringe adjacent to the mined-out high-grade core was studied using drill-core for thin-sections, polished-sections, x-ray diffraction, and chemical analyses.

An intrusive-extrusive "potassic"-rhyodacite porphyry is the major ore-hosting rock unit. Rhyolite and rhyodacite tuffs are less well mineralized. The major alteration types are two argillic assemblages (the expansible-clay facies and the more advanced kaolinite facies) and silicification. Alunitization commonly accompanies silicification and they comprise the most advanced alteration type found. Wall-rock alteration resulted from the interaction of wall rocks with acidic hydrothermal solutions. Hydrogen metasomatism occurred. The boundary between the two argillic facies is sharp, marked by the complete destruction of sanidine. The high-grade core was characterized by extreme silicification and is nonsymmetrically surrounded by the two argillic facies due to differential fracturing and thus variable permeability of the wall rocks. The presence of potassic clays (illite/smectite, rectorite) and the rarity of discrete illite or sericite suggest that temperatures during wall-rock alteration and mineralization never exceeded 200^o C.

The ore minerals in the low-grade fringe include sphalerite, galena, and a trace of chalcopyrite. The galena is argentiferous. Gangue minerals include pyrite, barite, quartz, and clays. Textures indicate that open-space filling was the dominant means of sulfide emplacement. Barite and pyrite deposition preceded galena and sphalerite. Galena and sphalerite were deposited in an overlapping series. Ore concentrations increase in the more intensely altered rocks. Fractures and leached phenocryst voids provided openings for ore mineralization. Sulfide precipitation created more acidic solutions locally and caused kaolinite facies alteration in the argillized fringe.

The Flathead mine exists in the immediate vicinity of an ancient volcanic vent. A hydrothermal convective cell existed during the waning stage of the vent's volcanic activity. Ore precipitation resulted by the mixing of metal-bearing solutions with meteoric water and perhaps also by reactions with sulfates. A "sodic"-rhyodacite porphyry flow capped the area after hydrothermal activity had ceased.

ACKNOWLEDGMENTS

Many thanks to the members of my committee:
Ian Lange (chairman), Gray Thompson, and Keith Osterheld, for their suggestions, guidance, and editing of the manuscript. I also thank Jack Wehrenberg for his assistance on the x-ray powder camera. I am indebted to Canadian Superior Mining and Exploration (U.S.) Ltd. for providing me access to the property, use of drill-core, and partial funding for the project. And last, a very special thanks to a real sweetheart of a girl, my typist and inspiration, Peggy Smith.

TABLE OF CONTENTS

	Page
ABSTRACT	ii
ACKNOWLEDGMENTS	iii
LIST OF TABLES	vii
LIST OF FIGURES	viii
CHAPTER	
I. INTRODUCTION	1
General Statement	1
Location	2
Previous Work	2
Mining History	2
II. REGIONAL AND LOCAL GEOLOGY	4
Belt Rocks	4
Igneous Rocks	6
III. ANALYTICAL WORK	8
Rock Sampling	8
Petrography	8
X-Ray Diffraction	11
Whole-Rock and Selected Metal Chemistry	12
IV. FLATHEAD MINE GEOLOGY	14
Porphyry Rock Nomenclature	14
Structure	17
Rock Descriptions	20
"Potassic"-Rhyodacite Porphyry	20

CHAPTER	Page
Macroscopic description	25
Petrography	26
Rhyolite and Rhyodacite Tuffs	28
Macroscopic description	28
Petrography	30
Extremely altered tuffs	31
"Sodic"-Rhyodacite Porphyry	31
Macroscopic description	32
Petrography	32
Discussion and Conclusions	33
Modes of emplacement	34
Fine-Grained Alteration	36
Discrete Smectite	36
Illite/Smectite	39
Rectorite	39
Discrete Illite or Sericite	41
Disordered Kaolinite	41
Quartz	43
Sulfates	43
Kalinite	43
Discussion	45
Ore Mineralization	46
Selected Metal Chemistry Discussion	47
Ore Control and Paragenesis	49

CHAPTER	Page
Depth of Formation	55
V. ALTERATION PROCESSES	56
Expansible-Clay Facies	57
Kaolinite Facies	59
Silicification	62
Equilibrium Diagrams	62
Anionic Metasomatism	66
Discussion	67
VI. THE VOLCANIC ENVIRONMENT	71
Precipitation of the Ore	72
VII. VOLCANIC SILVER DEPOSITS: A COMPARISON	74
VIII. SUMMARY AND CONCLUSIONS	82
Prospecting Suggestions	87
BIBLIOGRAPHY	89
APPENDIX	94

LIST OF TABLES

Table	Page
1. Whole-rock Chemistry Analyses	15
2. Average Whole-rock Values of Igneous Rocks .	16
3. X-ray Diffraction Results	37
4. Metal Chemistry Analyses	48
5. Volcanic Silver Deposits	75-76

APPENDIX TABLES

Appendix	Page
1. Drill-core Samples	95
2. Mineralogy of "Potassic"-Rhyodacites (Expansible-Clay Facies)	96-98
3. Mineralogy of "Potassic"-Rhyodacites (Kaolinite Facies)	99-100
4. Mineralogy of "Potassic"-Rhyodacites (Extremely Silicified Rocks)	101
5. Mineralogy of Rhyolite and Rhyodacite Tuffs .	102
6. Mineralogy of "Sodic"-Rhyodacites	103
7. Abbreviations Used	104

LIST OF FIGURES

Figure	Page
1. Location Map	5
2. Geologic Map	9-10
3. Experimental Phase Diagrams	18
4. Drill-hole Panels	21-24
5. Photomicrograph-Amphibole Ghost	29
6. X-ray Patterns for Smectite	38
7. X-ray Patterns for Rectorite	40
8. X-ray Patterns for Disordered Kaolinite	42
9. X-ray Pattern for Alunite and Quartz	44
10. Lead Migration from Sphalerite-Galena Vein	51
11. Sphalerite-Galena Vein with Open-space Fill	52
12. Barite with Interstitial Sphalerite	54
13. Mineral Paragenesis	55
14. Variation Diagrams	60-61
15. Experimental Equilibrium Diagrams	63
16. Hypothetical Equilibrium Diagrams	64
17. Genetic Model	83

CHAPTER I

INTRODUCTION

General Statement

Extensive hydrothermal alteration commonly occurs in volcanic rocks bordering epithermal silver deposits. The relatively cool wall-rocks present a significant temperature differential with the hydrothermal solutions. This disequilibrium results in reactions that typically produce widespread and conspicuous wall-rock alteration. Ore-mineralization and alteration often occur as conformable zones, but no obvious relation necessarily exists if hydrothermal solutions precede or post-date the ore-bearing phase of solutions.

I examined the alteration petrology at the Flathead mine. Argillic alteration and silicification are extensive. Macroscopic alteration mineralogy at the Flathead mine is a good guide to ore-mineralization because alteration accompanies mineralization, is more conspicuous than mineralization, and the richest ore occurs in the most intensely altered rocks. Detailed clay analysis is unnecessary for exploration because of the macroscopic aspects of the alteration. The characteristics (i.e., age, structural controls, alteration, ore and gangue minerals, ore textures) of the

Flathead mine are similar to other volcanic silver-bearing deposits.

Location

The Flathead mine is located in the Hog Heaven Range of northwestern Montana about 24 kilometers west of Flathead Lake. The main mine area is situated in the N $\frac{1}{2}$, SE $\frac{1}{4}$ of Sec. 17, T.25 N., R.23 W. The area is accessible via unpaved Sullivan Creek road off Montana Highway 28.

Previous Work

Shenon and Taylor (1936) authored an extensive report on the district and described the characteristics of the high-grade silver ore from the Flathead mine which has since been essentially mined out. Descriptions of volcanic rocks in the Hog Heaven mining district and adjacent areas were written by W. D. Page (Johns et al., 1963). A number of unpublished reports have been compiled by various mining companies.

Mining History

The Flathead mine is principally a silver-lead deposit. Discovery was made in 1928, though high-grade float was found in the vicinity in 1913 (Shenon and Taylor, 1936). Total production for the period 1928 - 1930 by the Anaconda Company and its lessees was about 20,000 tons of ore which yielded about 1,500,000 ounces of silver (75 oz./ton) (Shenon and Taylor, 1936). Estimated total production from 1928 - 1930 and 1934 - 1964 is 230,000 tons which yielded 6,700,000 oz. silver (\approx 30 oz./ton), 3,000 oz. gold (\approx .01 oz.

/ton), 23,000,000 lbs. lead ($\approx 5\%$), and 600,000 lbs. copper (.1%) (Krohn and Weist, 1977, p.52). No mining occurred between 1930 and 1934. Some production occurred between 1964 and 1976.

Various companies have leased the property from the Anaconda Company over the past several years. The Congden and Carey Co. conducted the diamond-drilling from which the drill core used in this study was obtained. Canadian Superior Mining and Exploration (U.S.) Ltd., which now leases the property, permitted the use of this core.

CHAPTER II
REGIONAL AND LOCAL GEOLOGY

The Flathead mine is situated in a semiarid region of moderate topography. The summit elevation of the hill north of the mine is 1397 m., and the Main Level adit of the mine is approximately 1241 m. in elevation, about 427 meters away horizontally. The principal drainage for the area, Sullivan Creek, is about .7 kilometers west of the mine at about 1097 m. Water is scarce here in the summer and Sullivan Creek amounts to little more than a trickle. Abundant pine and fir trees surround the area. Surface rock exposure in the main mine area is about 8%. Extensive bulldozer roadcuts have greatly enhanced the amount of rock exposure.

The Flathead mine is not the only mineralized deposit in the area (fig. 1). Approximately .4 km. to the east is the Mary Ann mine in the $W\frac{1}{2}$, $SW\frac{1}{4}$ of Sec. 16, T.25 N., R.23 W. About .8 km. to the west is the West Flathead mine in the $E\frac{1}{2}$, $SW\frac{1}{4}$ of Sec. 17, T.25 N., R.23 W. The Ole mine is located 1.4 km. to the west in the east central part of Sec. 18, T.25 N., R.23 W.

Belt Rocks

Precambrian metasedimentary rocks found in the district

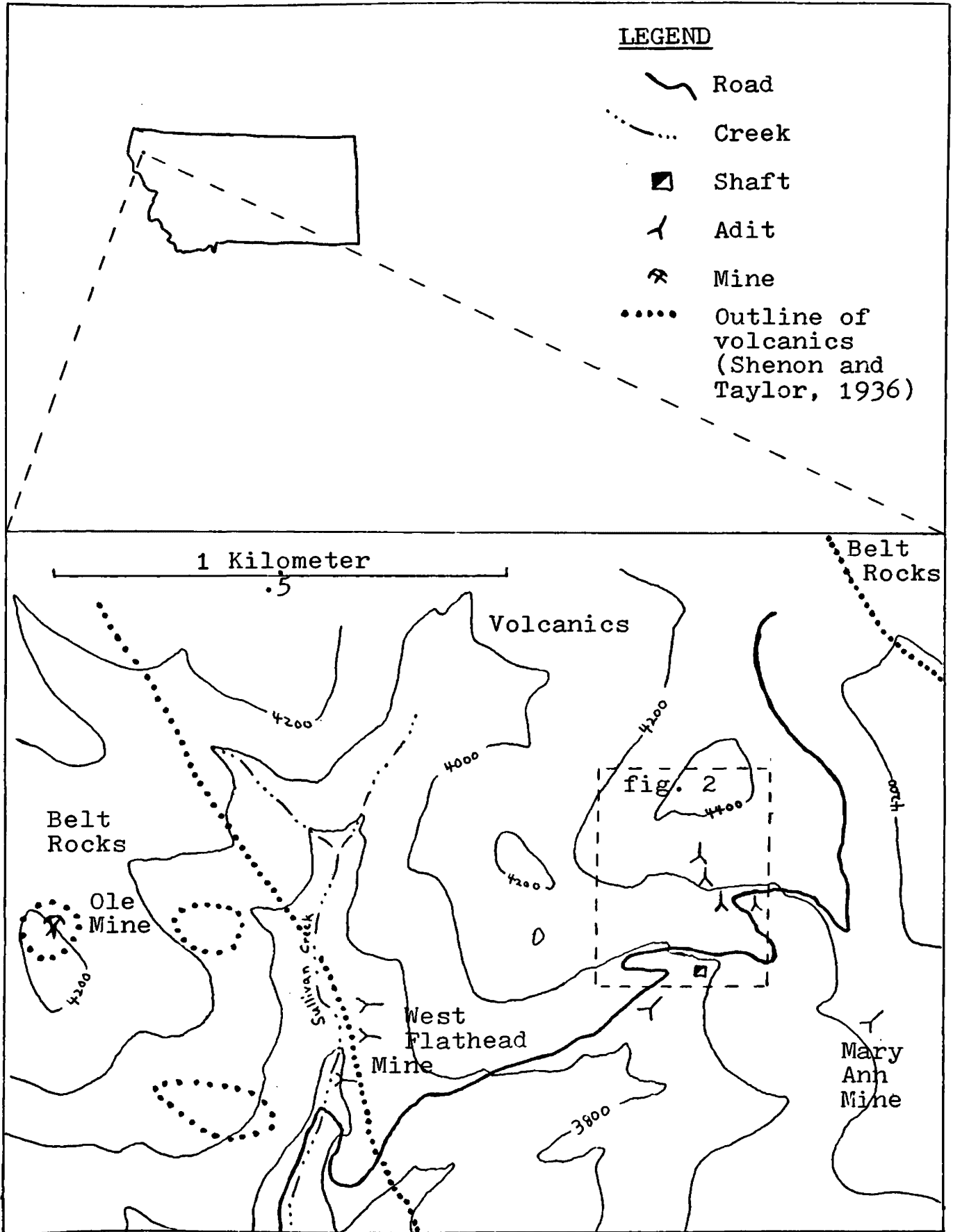


Fig. 1. Location map showing mines in the area. The Flathead mine is in fig. 2.

include at least two formations. Shenon and Taylor (1936) report exposures of the Ravalli group east, west and northwest of the Flathead mine. These rocks consist principally of greenish-grey to light-grey, thin-bedded argillite. The rock textures are the same everywhere. Harrison et al. (1974) mapped these rocks as the Burke formation. Northeast of the Flathead mine, Wallace group rocks occur (Shenon and Taylor, 1936). These rocks consist principally of relatively thin-bedded, noncalcareous, light-grey shale. Both formations are almost horizontal; no dips exceed 5° .

Belt formations are not found at the Flathead mine. However, numerous clasts of Belt rock are incorporated within the lithic porphyry and tuff units. Here they consist of light-grey to black argillite and, less commonly, quartzite.

Igneous Rocks

The Flathead mine is in Tertiary volcanic rocks. The igneous rocks of the region sporadically cover about 65 km²; outcrop is not continuous. The lack of continuity of the flows and tuffs led W. D. Page (Johns et al., 1963) to conclude that only the thicker valley-fill volcanics survived erosion.

In the same report, Page described andesite and latite porphyries, andesite, latite and trachyte tuffs, basalt, and intrusive quartz latite. Chemical analyses of glass-bearing rocks may reveal errors in rock naming. Shenon and Taylor (1936) named the rocks andesites and latites on the basis of

mineralogy. Page (Johns et al., 1963) concluded that rock suites of this type occur as late orogenic eruptions confined to a continental environment. They are not part of an extensive igneous province.

The precise age of volcanic activity is unknown. Tuffs are underlain by and interbedded with Tertiary lake bed deposits (Shenon and Taylor, 1936). Wisconsin age glacial-outwash terraces crosscut tuffs near Hubbert Reservoir (Johns et al., 1963). These occurrences bracket the age of these rocks.

CHAPTER III
ANALYTICAL WORK

Rock Sampling

In order to distinguish hydrothermal alteration from surface weathering products, it was necessary to obtain samples below the zone of oxidation. This was accomplished through the use of nx drill core. Most of the samples came from five drill holes, each approximately 213 meters deep. Drill-hole locations are plotted on the geologic map (fig. 2). Sample locations within the hole are listed in appendix 1. The drill holes selected for study create a 325 meter long east-west, 3-hole panel and an intersecting 460 meter long north-south, 3-hole panel. The panels lie adjacent to the former rich ore zone.

Petrography

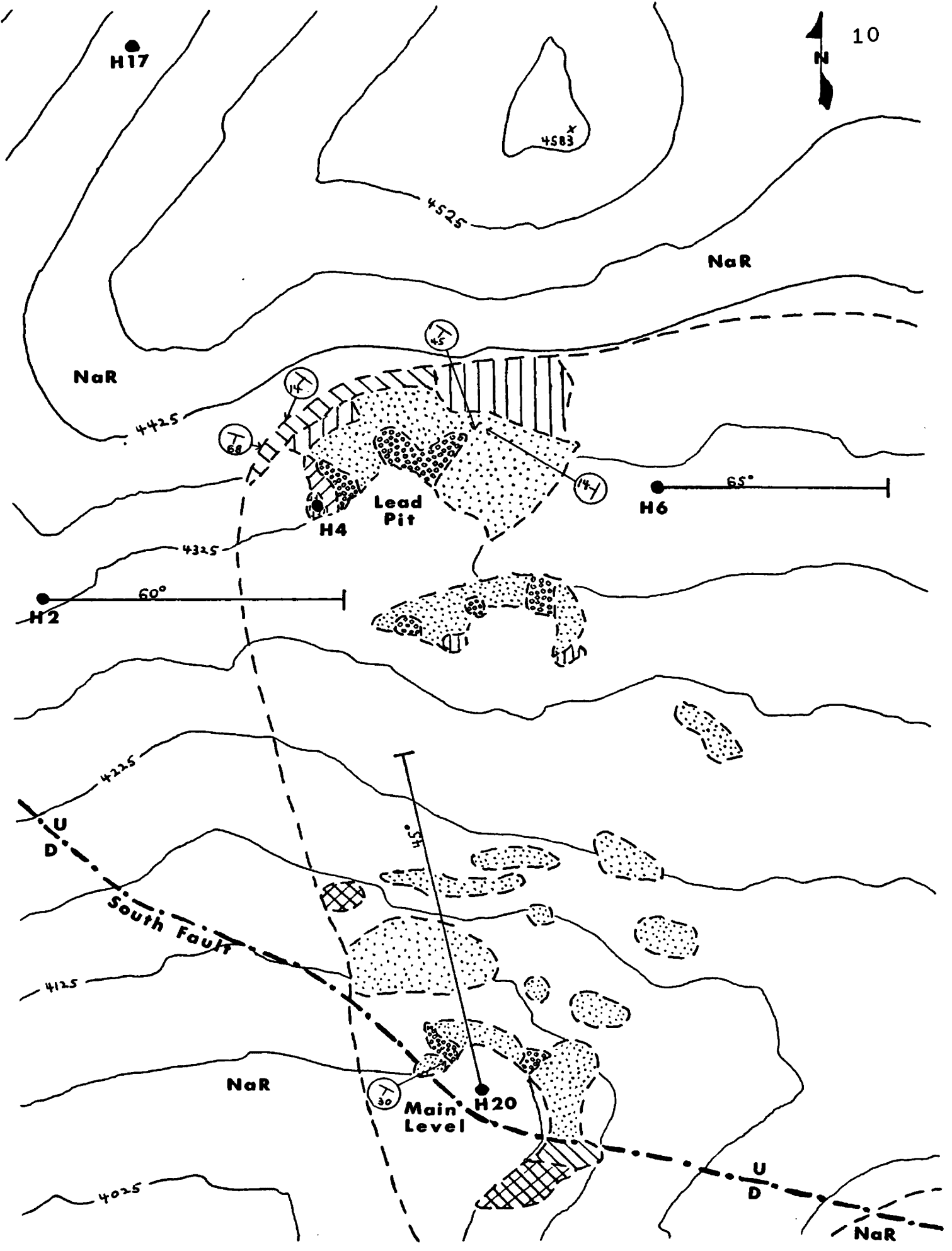
Fifty-seven thin-sections were examined petrographically (see appendix 2-6) to determine lithologies, hypogene minerals, and general alteration assemblages. Samples were selected to cover the full range of rock types and depth. Many thin-sections were stained with sodium cobaltinitrite to distinguish sanidine (potassium feldspar). This procedure also distinguished potassium-bearing clays from silici-

**FIGURE 2 GEOLOGIC MAP - FLATHEAD MINE
LEGEND**

-  "Sodic"-Rhyodacite porphyry
- Altered-rock outcrops (Expandable-Clay Zone)
-  "Potassic"-Rhyodacite porphyry
-  Lithic "Potassic"-Rhyodacite porphyry
-  Tuff
- Altered-rock outcrops (Kaolinite Zone)
-  "Potassic"-Rhyodacite
-  Lithic "Potassic"-Rhyodacite porphyry
-  Tuff
-
-  Intensely silicified porphyry
-  Contacts
-  Fault (trace by Canadian Superior Ltd.)
- H4** Drill hole-w/angles if not vertical
-  Strike and dip of beds-location pinpointed

 200 ft.

 100m.



fication in the groundmass.

Twelve samples were polished for examination with reflected light. These samples contained the greatest amounts of sulfide minerals and barite.

X-Ray Diffraction

Fine-grained mineral recognition was based primarily on x-ray diffraction. Fifty-three samples were analysed (see table 3, p. 34) and included the full range of rock types, depth, and proximity to sulfide minerals.

Clay minerals were released from the rocks by hand-crushing samples with a steel mortar and pestle. The fines produced were mixed with deionized distilled water and further disaggregated with an ultrasonic probe for four minutes. A tiny amount of Calgon was added to prevent flocculation. The slurry was then centrifuged to settle the greater than 2 micron size fraction. The less than 2 micron size fraction that remained in suspension was then placed on glass slides with an eyedropper. The samples were allowed to dry. This preparation caused the sheet silicates (clays) with platy morphology to orient themselves parallel to the glass slide as the water evaporated. Oriented samples give stronger basal peak reflections. Clays with expansible layers were identified after samples were subjected to an ethylene glycol atmosphere for 24 hours. Where rocks lacked clay, random (unoriented) samples were prepared by sprinkling dried and powdered fractions on a petroleum jelly-coated slide.

The prepared samples were analysed with a Norelco x-ray diffractometer with a scanning goniometer using Ni-filtered $\text{CuK}\alpha$ radiation. Transformer-generator settings were at 30 kv and 20 ma. Oriented samples were scanned thru the $32^\circ - 0^\circ 2\theta$ range. Scanning speed was $\frac{1}{2}"/\text{min}$. Transmission and receiving slit combination was $1^\circ - 1^\circ$.

Whole-Rock and Selected Metal Chemistry

Nine rocks taken from the drill-core and one surface sample (P-UP) were chosen for whole-rock chemical analysis (see table 1, p. 13). The drill-core samples were also analysed for Ag, Cd, Co, Cu, Ni, Mo, Pb, Sb, V and Zn (see table 4, p. 45). Sample H4-18 was also analysed for Bi. Samples were selected after preliminary petrographic and x-ray analysis so that all lithologic, ore and alteration types were included. To avoid contamination, rocks with lithic fragments were not selected except for sample H4-18 which was chosen for its ore content. Chemical analyses were performed by Technical Services Laboratories (TSL), Mississauga, Ontario.

Whole-rock chemistry samples were fused with a borate-carbonate flux and dissolved in nitric acid. Major oxides were determined by ICAP (inductively coupled argon plasma) (Skoog and West, 1980, p. 340-342) using International Reference Standards prepared with the samples. The precision of chemical analysis is $\pm 2\%$ of the amount listed for each element (personal communication, TSL).

Metal-chemistry samples were dissolved and dried several times in hydrofluoric aqua-regia before redissolving in HCl. Metals were determined by atomic absorption (Skoog and West, 1980). The precision of each analysis is $\pm 3\%$ except near limits of detection (a few ppm) where precision is $\pm 25\%$ (personal communication, TSL).

CHAPTER IV
FLATHEAD MINE GEOLOGY

Porphyry Rock Nomenclature

Chemical analysis is needed to name rocks with high glass content. Silica percentages are commonly used in making chemical designations for glass-bearing rocks (Hyndman, 1972). Aluminum analyses may also be useful due to the comparative immobility of that species in hydrothermal alteration and weathering.

It is somewhat misleading to compare the chemical values from the altered rocks of the Flathead mine to fresh rock values in attempting to classify the rocks on the basis of chemical composition. Each analysis represents relative amounts of the various elements so that removal of constituents will result in increases for those not removed. The lack of original crystalline material and compositional ambiguities due to alteration permit only a general classification.

Whole-rock compositions of study-area rocks (table 1) are compared with average whole-rock values for common volcanic rocks (table 2). Silica percentages for study-area rocks are a few percent higher than the dacite average.

MAJOR OXIDES - %

	"Sodic"-Rhy.		"Potassic"-Rhyodacites						Tuff	
			Expansible-Clay Facies			Kaolinite Facies				
	<u>H2-1</u>	<u>P-UP</u>	<u>H4-3</u>	<u>H20-8</u>	<u>H20-10</u>	<u>H4-16*</u>	<u>H4-18*</u>	<u>H20-12*</u>	<u>H4-21</u>	<u>H17-23</u>
SiO ₂	67.58	67.93	68.89	63.22	65.14	39.52	59.85	54.05	69.62	70.03
TiO ₂	0.38	0.43	0.49	0.46	0.56	0.51	0.37	0.43	0.45	0.47
Al ₂ O ₃	15.99	16.31	14.51	15.05	15.95	15.42	7.47	17.71	12.90	16.67
Fe ₂ O ₃	2.58	2.32	2.98	4.08	2.18	5.65	5.20	4.94	5.54	3.28
MnO	0.02	0.01	0.03	0.40	0.14	0.02	0.01	0.03	0.02	0.02
MgO	0.32	0.14	0.48	0.93	0.97	0.10	0.07	0.14	0.11	0.09
CaO	1.85	1.99	1.07	1.96	2.28	0.89	0.48	0.74	0.76	0.42
Na ₂ O	4.84	4.46	1.18	0.23	0.00	0.00	0.00	0.00	0.00	0.00
K ₂ O	2.99	3.19	5.57	6.29	5.82	0.19	0.11	0.33	0.11	0.23
P ₂ O ₅	0.29	0.33	0.28	0.37	0.53	0.74	0.55	0.54	0.27	0.19
LOI	1.63	2.43	4.05	4.64	4.12	12.23	7.37	9.90	8.36	8.55
Total	99.48	99.95	99.95	97.64	97.68	75.28	81.49	88.81	98.13	99.96

*NOTE: Totals for H4-16, H4-18 and H20-12 are low and duplicate analyses give similar values. Part of the problem could be that sulfides may form sulfates during ignition resulting in low values for LOI (loss on ignition). See table 4 for metal contents.

Analyses performed by Technical Service Laboratories, Mississauga, Ontario.

Table 1. Whole-rock chemistry of selected Flathead mine samples.

	<u>Rhyolite</u>	<u>Dacite</u>	<u>Latite</u>	<u>Andesite</u>
SiO ₂	72.82	65.01	61.25	57.94
TiO ₂	0.28	0.58	0.81	0.87
Al ₂ O ₃	13.27	15.91	16.01	17.02
Fe ₂ O ₃	1.48	2.43	3.78	3.27
FeO	1.11	2.30	2.07	4.04
MnO	0.06	0.09	0.09	0.14
MgO	0.39	1.78	2.22	3.33
CaO	1.14	4.32	4.34	6.79
Na ₂ O	3.55	3.79	3.71	3.48
K ₂ O	4.30	2.17	3.87	1.62
H ₂ O ⁺	1.10	0.91	1.09	0.83
H ₂ O ⁻	0.31	0.28	0.57	0.34
P ₂ O ₅	0.07	0.15	0.33	0.21
CO ₂	0.08	0.06	0.19	0.05
Total	99.96	99.78	99.83	99.93

Table 2. Average whole-rock chemical values (Le Maitre, 1976).

However, silica values for study-area rocks may be low because hydrothermal alteration (Meyer and Hemley, 1967) and weathering (Goldich, 1938; Krauskopf, 1979, p. 82) tend to lower silica percentages. Aluminum values for study-area rocks appear too high for rhyolite. Silica and aluminum values indicate that all of the porphyritic rocks at the Flathead mine are rhyodacites (Streckeisen, 1979).

Two separate porphyry units were mapped (fig. 2) because of their dissimilarities in feldspar phenocryst mineralogy. "Potassic"-rhyodacite is used for the older porphyry units that are intensely altered and contain more and larger sanidine phenocrysts. "Sodic"-rhyodacite is used for the younger, comparatively fresh porphyry units in which sanidine is subordinate to plagioclase and is not of large size. These are, respectively, the porphyritic latites and porphyritic andesites of Shenon and Taylor (1936) who named the rocks solely on phenocryst mineralogy.

Fig. 3 illustrates the crystallization of each rhyodacite melt. Crystallization paths are curved because of the changing composition of the melts with crystallization. Quartz did not crystallize because rapid cooling of the melts on extrusion apparently did not permit attainment of the quartz cotectic.

Structure

The rhyodacite porphyry units outcropping in the Flathead mine area show few contacts. Thin interbeds of tuff

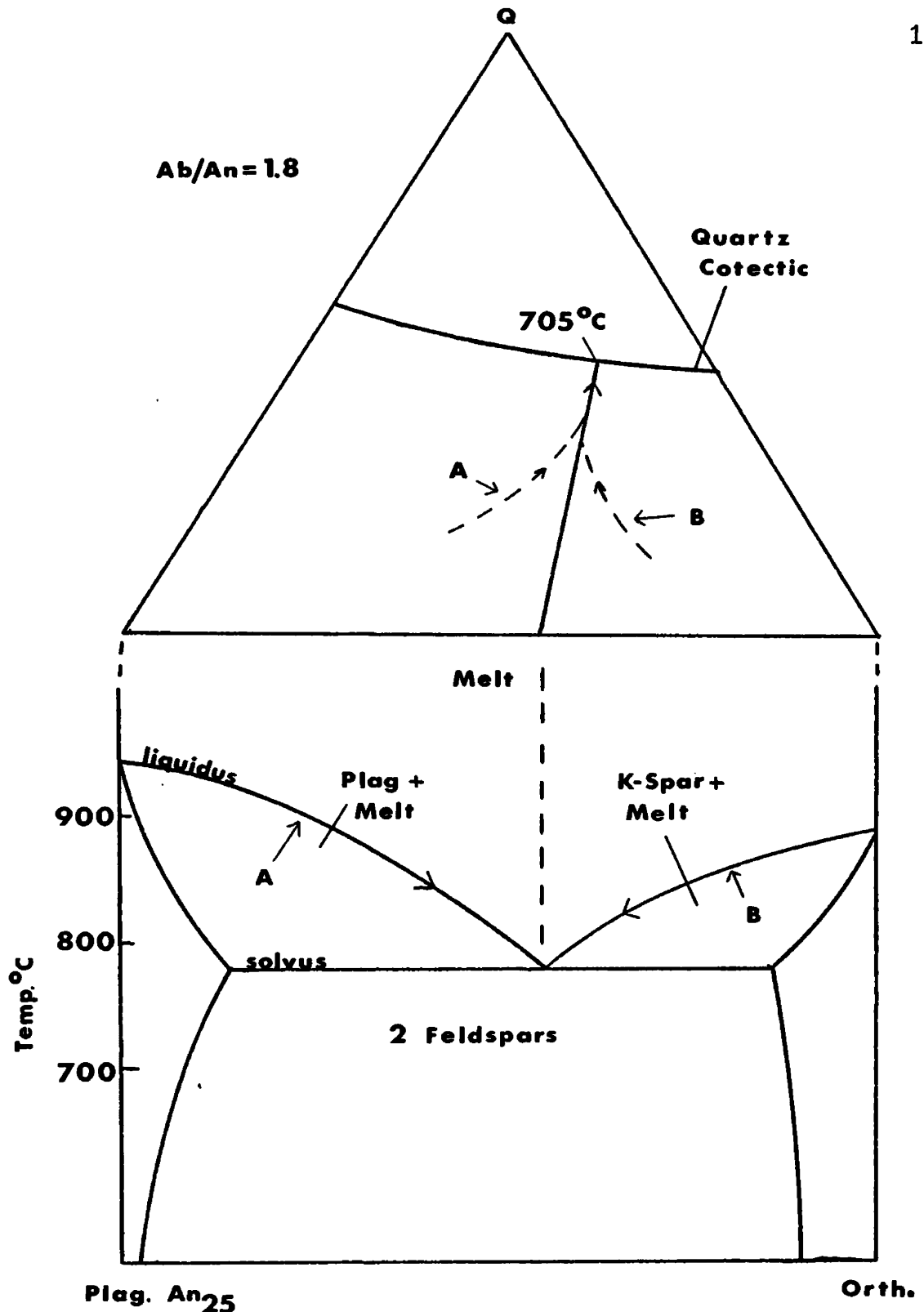


Fig. 3. Correlation of experimental phase diagrams depicting crystallization of plagioclase and orthoclase melts at 2000 bars P_{H_2O} . The "sodic"-rhyodacite melt is represented by the path to the left of the 2 feldspar cotectic (A), the "potassic"-rhyodacite melt to the right (B). The binary diagram (Hyndman, 1972, p. 134) would require additional calcium to perfectly match the plagioclase of the ternary diagram (von Platen, 1965). That would expand the solvus and raise the liquidus.

demonstrate the attitude of the "potassic"-rhyodacite in some areas and the contact surface with the overlying "sodic"-rhyodacite is easily observed in the Lead Pit area. Attitudes vary widely though southerly dips of 14° to 45° predominate. The attitude of the overlying "sodic"-rhyodacite flow is topographically controlled. Offset beds and the small scale over which attitudes vary in the tuffs interbedded with the "potassic"-rhyodacite cannot be attributed to topographic variations. They reflect post-emplacement movements in addition to topographic constraints.

Although fracturing is present in the mine exposures, there is little surface expression to indicate major faulting. The South Fault (fig. 2) is the notable exception. However, underground mapping indicates extensive faulting with displacements predominantly from one to two meters. Larger faults with "doughy" gouge may have displacements from several 10's to possibly 100's of meters (personal communication, Mike Wilson, 1981).

No slickensides are apparent in the drill-core but small brecciated zones (≤ 5 cm. wide) are present. Fractures with small offsets (≤ 5 mm.) occur in core samples.

Fracturing has played a large part in the ore-forming processes. Sulfides and sulfates occur largely in veins. Fractures acted as avenues of transport for ore-bearing solutions and sites for deposition. These fractures may be associated with faulting.

Figs. 4a. and b. present the drill-hole "panels" in cross-section though distances between holes are not to scale. Inability to reliably correlate drill-hole stratigraphy is attributed to a large variance and non-persistence of rock units and perhaps faulting.

Rock Descriptions

"Potassic"-Rhyodacite Porphyry

The porphyritic "potassic"-rhyodacite which hosts the ore at the Flathead mine was believed to be intrusive by Shenon and Taylor (1936). However, interbeds of tuff occur as continuous layers within the porphyry indicating the rocks are extrusive. This is well-illustrated at the north-east edge of the Lead Pit. W. D. Page (Johns et al., 1963) reports that tree trunks were found within the rock inside the mine which demonstrate an extrusive origin for the "potassic"-rhyodacite. Page also states that Anaconda Company underground maps show dikes and sills in deeper workings indicating some of the rocks are intrusive.

Some porphyry units (e.g., on west side of Lead Pit) contain volcanic and Belt rock fragments. Well-rounded Belt fragments represent either an earlier period of stream-reworking before incorporation in the flow or movement in volcanic vents (i.e., breccia pipe). Lithic and non-lithic units are probably separate flows; they are not described separately because their characteristics are the same except for the lithic content.

Fig. 4a. Drill-hole sections constituting a north-south panel. Pattern on the left of the section depicts rock type, pattern on the right depicts alteration. Hole H20 is an angle-hole, but its section is shown corrected to vertical depth. The sections are aligned according to elevation. Numbers on the right side of the section refer to sample locations. For sample depths see Appendix 1; drill-hole locations are on fig. 2.

Scale: 1 inch = 70 feet

1 cm. = 8.4 meters

LEGEND



"Potassic"-Rhyodacite Porphyry



Lithic "Potassic"-Rhyodacite Porphyry



Tuff



Intensely Silicified Rocks (rock type unknown)



Kaolinite Facies



Expansible-Clay Facies

Fig.4b. Drill-hole sections constituting an east-west panel. Pattern on the left of the section depicts rock type, pattern on the right depicts alteration. Holes H-2 and H-6 are angle-holes, but sections are shown corrected to vertical depth. The sections are aligned according to elevation. Numbers on the right side of the section refer to sample locations. For sample depths see Appendix 1; drill hole locations on Fig. 2.

Scale: 1 inch = 70 feet
1 cm. = 8.4 meters

LEGEND

-  "Sodic"-Rhyodacite Porphyry
-  "Potassic"-Rhyodacite Porphyry
-  Lithic "Potassic"-Rhyodacite Porphyry
-  Tuff
-  Intensely Silicified Rocks (rock type unknown)
-  Kaolinite Facies
-  Expansible-Clay Facies

The porphyritic "potassic"-rhyodacite at the Flathead mine developed some distinct mineralogic characteristics reflecting the degree of hydrothermal alteration. The most useful guide to the intensity of alteration is the presence or absence of sanidine. Sanidine is the most resistant mineral in the rhyodacite except zircon which is present in minor amounts. It is important, therefore, to note differences between rocks with completely altered sanidine and rocks with fresh sanidine. Fresh "potassic"-rhyodacite was not found in the vicinity of the Flathead mine.

Macroscopic description. Altered phenocrysts of plagioclase and sanidine are now patches of white clays set in a light to dark-gray microcrystalline matrix. Non-altered sanidine in the rhyodacite appears glassy. Fresh plagioclase, which is rare, is white. The color contrasts give the rock an overall spotted appearance. Surface rocks commonly contain cavities due to weathered-out clays. The oxidation of iron has colored the rocks shades of red, brown, and yellow, especially intensely at the surface.

The sanidine phenocrysts are larger than the plagioclase phenocrysts. The largest fresh sanidine found was 3.5 cm. long, but altered sanidine up to 6 cm. long is also found. The plagioclase is commonly less than .4 cm. long. Sanidine and plagioclase occur as euhedral to anhedral crystals with sharp boundaries. Together they comprise about 50% of the rock. No other rock-forming minerals are visible.

Sphalerite and galena appear where sanidine becomes rare or absent due to replacement. However, pyrite is commonly found even with an abundance of fresh sanidine.

Pits, representing leached crystal sites, are present in rocks that underwent extreme silicification. This silicified rock is commonly rich in barite and pyrite.

The rock fragments in the lithic "potassic"-rhyodacite units are either Belt metasediments or local volcanic rocks. Belt fragments are mostly light or dark-grey argillites. Quartzite is rarer. The volcanic fragments are altered porphyries and fine-grained tuffs. The Belt fragments generally are rounded, whereas the volcanic fragments are generally more angular. The largest clast found was 4 cm. across; commonly sizes were less than .5 cm. in diameter.

Petrography. In thin-sections, the "potassic"-rhyodacites are dominated by fine to very fine-grained (unrecognizable) low-birefringent minerals. They display a "salt and pepper" texture with little or no intergranular change in relief. These replacement/alteration minerals are quartz and clays; they comprise between 70 and 95% of the rocks. Quartz in the groundmass may be a devitrification product of volcanic glass. The porphyritic character of the rocks generally survived alteration. Various crystals and crystal relics are scattered in a fine-grained matrix with no preferred orientation of the crystals or the matrix except sample H2-17, which contains amphibole ghosts that have a

preferred orientation.

Appendices 2, 3, and 4 list the mineralogy of "potassic"-rhyodacite samples from the Flathead mine. Fresh sanidine never exceeded 25% of the rock. Subhedral to anhedral crystals are dominant. Carlsbad twins are commonly developed. In sample H17-13, sanidine is slightly zoned. A number of the smaller sanidine crystals are broken. The sanidine generally has sharp crystal boundaries but some are embayed by secondary fine-grained matrix minerals.

Fresh plagioclase is rare in the "potassic"-rhyodacite. Commonly it occurs only in trace amounts. Crystals are dominantly subhedral to anhedral. Albite twinning is nearly ubiquitous; anorthite content is An_{34} - An_{38} (andesine). Some of the plagioclase crystals have sharp boundaries; others have altered edges. A few are slightly embayed. Some of the crystals are broken.

A trace of biotite and magnetite was found in these rocks. The only other original minerals found were minor amounts of euhedral zircon and apatite. Zircon persists even after complete sanidine destruction. Some small anhedral quartz crystals may be primary, but most, if not all, are secondary. They commonly have undulose extinction.

Leucoxene is a common alteration mineral in these porphyry units. It regularly borders silicified or argillized mafic minerals, more rarely replacing the whole crystal. It is an opaque mineral that yields a creamy white color in

reflected light. Many samples reveal well-preserved ghost crystals replaced by leucoxene. Distinct hexagonal amphibole ghosts show leucoxene replacement along crystal outlines and 120° cleavage traces (fig. 5). This indicates the original presence of the titanium-bearing amphibole kaersutite. Aoki (1963) and Heinrich (1965) testify to its common occurrence in felsic extrusive rocks. Other titanium minerals are partially replaced by leucoxene. Rhombohedral ghosts represent sphene and possibly ilmenite.

Hematite and limonite are pervasive in many samples. Pyrite is commonly disseminated throughout the "potassic"-rhyodacite. Some are surrounded with limonite. Very small amounts of sericite are found, commonly occurring with pyrite. A few samples have up to 6% carbonate. Chemical analysis of sample H20-8 shows an anomalous amount of manganese. However, calcium is also high. The carbonate could be rhodochrosite, calcite or a solid solution of the two (Palache et al., 1951). The amount of sulfide mineralization (galena, sphalerite) and barite is inversely proportional to the amount of fresh sanidine. Alunite and jarosite occur with barite and sulfide minerals in a few samples. The lithic "potassic"-rhyodacite porphyry units contain sericite/muscovite confined to the clasts.

Rhyolite and Rhyodacite Tuffs

Macroscopic description. Recognition of these units in the field and in drill core is essentially based on the lack

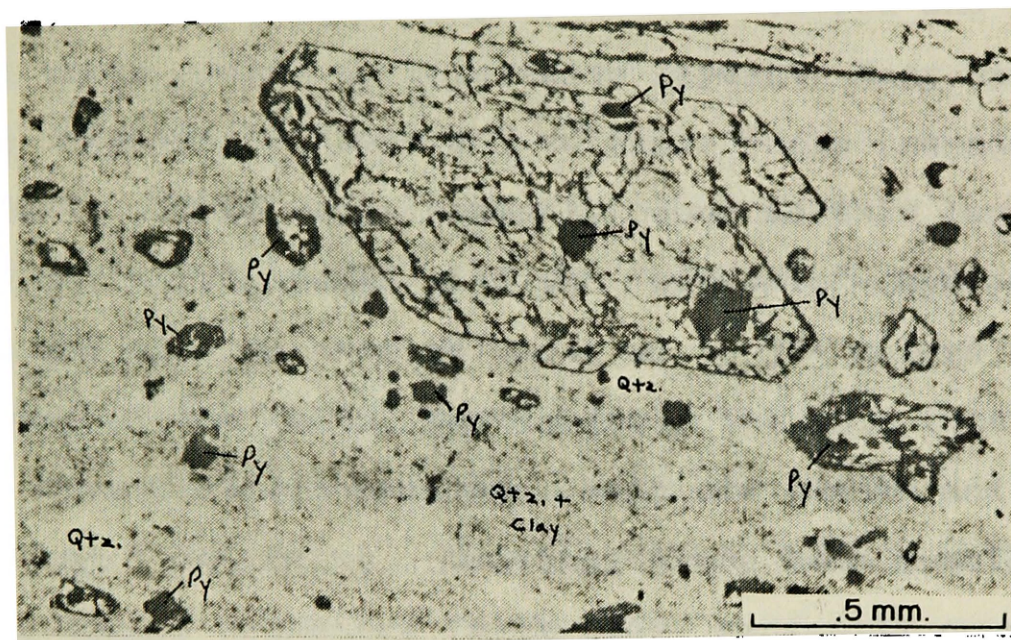


Fig. 5. Photomicrograph of altered "potassic"-rhyodacite (sample H2-17) showing amphibole (kaersutite) ghost replaced by leucoxene along outline and cleavages. Lighter patches are quartz. Darker patches are clays (kaolinite and rectorite) plus quartz. Leucoxene and pyrite are black.

of porphyritic character. They are moderately to well-sorted and generally too fine-grained to distinguish any minerals with the rare exception of small, glassy sanidine crystals. The rocks are grey to tan colored and some have small white grains or thin white layers. Many have grey to white fragments of Belt and volcanic rocks (rounded to angular). These rocks commonly occur as thin layers (≤ 20 cm.) interbedded with the "potassic"-rhyodacite porphyry and also as massive units up to 30+ meters thick.

Many of the units, particularly the thin interbedded ones, have distinct bedding. Beds are planar and generally less than 5 cm. thick. Commonly these beds consist of fining-upward sequences (silt-clay, sand-silt couplets). At least one sample (H17-9) has small-scale cross-bedding. These bedding characteristics suggest deposition in water. Sample H17-1 has a swirling lenticular "flow structure" texture.

Petrography. Appendix 5 lists the mineralogy of tuff samples from the Flathead mine. Thin-sections reveal varying amounts of original crystalline material (4-50+%). Quartz is present as both a primary and secondary mineral. The groundmass of these rocks consists of extremely fine-grained low-birefringent minerals. Quartz is the major constituent but clays are also present as indicated by x-ray diffraction.

Sanidine and plagioclase occur as anhedral to subhedral crystals, rarely exceeding 1 mm. in diameter. The plagio-

class has albite twins. The other primary minerals are zircon and a trace of biotite.

Hematite and limonite are present in some samples. Half of the samples contain leucoxene; in sample H17-14 it replaces rhombohedral crystal ghosts. Sericite is present in minor amounts, confined primarily to foreign lithic fragments. Barite replaces feldspar in sample H17-1 and fills feldspar casts in sample H17-14. Pyrite is commonly disseminated in small amounts.

Extremely altered tuffs. A group of rocks with silt-size grains are classified tentatively as rhyolite and rhyodacite tuffs (e.g., samples H4-17, H6-11, H17-15, H17-23). They are composed predominantly of quartz and clay. Some pyrite, magnetite, leucoxene, and sericite are present. They probably represent tuffs whose textures were completely obliterated by hydrothermal alteration. Fine-grained tuffs alter readily because of their high porosity, large particle surface area and the instability of glassy fragments (Williams et al., 1954).

These units occur as thin interbeds (15-60 cm.) and massive units. Pyrite (up to 10%) is commonly concentrated in stringers and layers as well as disseminated. Sphalerite is present in sample H17-23.

"Sodic"-Rhyodacite Porphyry

Capping the hills and covering the immediate area of the Flathead mine is the younger "sodic"-rhyodacite porphyry.

Charred organic remains mark the contact with the tuffs in the northwest corner of the Lead Pit and indicate an extrusive origin.

Macroscopic description. White phenocrysts of plagioclase and lesser amounts of glassy sanidine are set in a light-grey to light-brown microcrystalline matrix. The phenocrysts comprise about 35% of the rock and are regularly less than 1 cm. long. A more coarsely porphyritic unit to the east has larger sanidine phenocrysts. Small black specks of biotite are scattered throughout. The "sodic"-rhyodacite has a "fresher" appearance than the "potassic"-rhyodacite. There are no soft clays replacing the feldspar phenocrysts. Green clays (probably nontronite) partly replace the matrix and biotite and make up about 10% of the rock.

Petrography. Primary crystalline material makes up 35-45% of the rock. Appendix 6 lists the mineralogy of "sodic"-rhyodacite samples from the Flathead mine. The groundmass consists of extremely fine-grained low-birefringent minerals consisting of clays (and feldspar?) with lesser amounts of quartz.

Plagioclase phenocrysts are euhedral to anhedral with sharp crystal boundaries. Albite twinning is abundant, carlsbad and pericline twins are rare. Plagioclase composition averages about An₃₈ (andesine). Some of the crystals are zoned. Many of the plagioclase grains have grown together

(glomerocrysts); a few are broken.

Sanidine comprises 1-6% of the rock. However, potassium values from table 1 ($\approx 3\%$) suggest more could have formed if given time to crystallize. Crystals are commonly subhedral to anhedral. Some sanidine crystals are enclosed in plagioclase; others enclose plagioclase.

Biotite makes up about 2% of the rock and occurs as euhedral to anhedral crystals less than 1 mm. long. A few grains in sample H2-1 are bent. Sphene generally makes up less than 1% of the rock, its borders commonly altered to leucoxene. Amphibole ghosts replaced by leucoxene along cleavages are rare. Magnetite with partial hematite replacement accounts for 2% of the rock. Apatite and zircon occur in small amounts. No pyrite or other sulfide mineralization exists in these rocks.

Discussion and Conclusions

The lack of sulfide mineralization and lack of unequivocal hydrothermal alteration in the "sodic"-rhyodacite suggests this unit post-dates the ore-forming processes. Alteration in this unit is attributed largely to weathering because of: 1) the lack of distinct hydrothermal minerals including sulfides; 2) fresh euhedral plagioclase and biotite "books"; 3) the low magnesium values from table 1 (H2-1, P-UP) are consistent with chemical changes upon weathering (Goldich, 1938); and 4) these rocks still have a high sodium content (hydrothermal alteration in the

"potassic"-rhyodacite leached sodium first and foremost in plagioclase destruction). The "sodic"-rhyodacite overlies tuffs and "potassic"-rhyodacite with advanced argillic alteration. Were the "sodic"-rhyodacite present during alteration of the other volcanics, the "sodic"-rhyodacite would show evidence of a more intense alteration (e.g., propylitic).

In order of increasing resistance to hydrothermal alteration and weathering, the primary minerals of the rhyodacites and rhyolites are: 1) amphibole (kaersutite); 2) biotite and sphene; 3) plagioclase (andesine); 4) sanidine and apatite; and 5) zircon.

Modes of emplacement. The interbedded tuffs with fining-upward sequences were probably deposited in "quiet" water after flows dammed local drainages. This origin is favored over direct air-fall deposition because the cross-beds in other interbedded tuffs suggest water deposition. Aeolian activity would probably stir up the ash and not form cross-beds. Ground-surge eruptions commonly display cross-beds (Sparks et al., 1973) but they characteristically show a wide variation in grain size and contain lithic fragments unlike the couplets and cross-beds of the Flathead mine tuffs.

The "sodic"-rhyodacite and much of the "potassic"-rhyodacite at the Flathead mine are extrusive as described earlier. Lack of bedding and poor sorting suggest an air-fall origin is unlikely. Field evidence is inconclusive in differentiating between pyroclastic and lava flows at the

Flathead mine.

Microscopic criteria for the recognition of pyroclastic ash-flows (Ross and Smith, 1961) includes:

- 1) Glass shards; commonly tricuspidate, U or Y-shaped.
- 2) Pumice fragments.
- 3) Eutaxitic structure - a foliate texture that resembles flowage due mainly to the flattening and compaction of glass shards and pumice fragments upon welding.
- 4) Axialitic structure - a devitrification texture with parallel intergrowths of feldspar and cristobalite growing perpendicular to glass or pumice walls and radiating inward.

Lava flows have less distinctive characteristics for identification. Williams et al. (1954) contend that laterally-continuous turbulent or fluidal lamination denotes lava flows and that perlitic cracks develop in glassy magmas which absorb water when cooling. Glomerocrysts might indicate a non-explosive eruption (Vance, 1969).

Criteria necessary to determine the origin of the porphyritic rhyodacites was not observed. Extensive alteration in the "potassic"-rhyodacites probably obliterated textural criteria. Perhaps both ash-flows and lava flows are represented. However, in the "sodic"-rhyodacites, the lack of distinct ash-flow textures suggest a lava-flow origin since the rocks did not undergo the intense hydrothermal alteration to erase those textures. The "sodic"-rhyodacite also contains feldspar glomerocrysts.

Fine-Grained Alteration

Table 3 lists the minerals distinguished by x-ray diffraction in the different rock types. If the relative abundance of each component was obvious it is indicated. Generally, comparison of peak intensities cannot give reliable estimates of abundances. However, gross differences in peak heights indicate primary versus subordinate components.

Discrete Smectite

A few clay samples are fully-expandible smectites. Smectite diffraction patterns show expansion of the basal d-spacing (001) to about 17.7\AA upon glycolation. An integral series of basal d-spacings follows. 100% expansibility (fig. 6) is determined using the peaks in the vicinities of 15.5 and $26^\circ 2\theta$ (Sroden, 1980).

The "sodic"-rhyodacite clays and sample H17-13 may also be fully-expandible smectites. However, the critical peaks for determining expansibility by Sroden's (1980) method were not resolved. These clays are tentatively identified as highly expandible ($\geq 80\%$) mixed-layer illite/smectites using the combined 001/002 peak method of Reynolds and Hower (1970). This method is susceptible to over 30% error due to particle size effects (Reynolds and Hower, 1970) and variable glycol thickness values (Sroden, 1980). Sample H6-6 (fig. 6) showed 100% expansibility using the method of Sroden (1980), yet only 65% expansibility by the method of Reynolds and Hower (1970).

"Sodic"- Rhyodacite	"Potassic"-Rhyodacite		Tuffs	
	(w/Sanidine)	(no Sanidine)	(w/Sanidine)	(no Sanidine)
H2-1: Smec (100%)	H2-2: Qtz	H2-4: Kaol	H2-3: Ill/Smec > Rect + Kaol trace: Illite or Sericite	H6-11: Qtz > Kaol
WP-7: Ill/Smec (90%)	H2-9: Rect	H2-15: Kaol + Qtz		H17-14: Qtz + Alunite + Jarosite
SD: Ill/Smec (80%)	H2-17: Rect (22%) + Kaol	H2-20: Kaol		
P-UP: Ill/Smec (80%)	H4-3: Ill/Smec (60%) + Kaol	H4-9: Kaol	H4-1: Ill/Smec + Kaol	H17-17: Qtz + Kaol
PF: Ill/Smec (90%)	H4-6: Qtz	H4-21: Kaol + Qtz	trace: Illite or Sericite	H17-25: Kaol + Illite or Sericite
C: Ill/Smec (80%)	H4-7: Qtz	H6-1: Kaol		
	H4-11: Kaol + Qtz	H6-5: Kaol	H17-3: Ill/Smec > Kaol	
	H4-12: Qtz	H6-8: Kaol	H17-9: Qtz > Kaol	
	H4-15: Qtz	H6-9: Kaol > Qtz		
	H6-6: Smec (100%) Kaol	H6-15: Qtz		
	H6-18: Qtz	H6-17: Qtz > Kaol		
	H6-21: Kaol > Rect	H17-16: Kaol + Qtz		
	H17-6: Ill/Smec + Kaol	H17-21: Qtz + Kaol		
	H17-12: Smec (100%) > Kaol	H20-2: Kaol		
	H17-13: Ill/Smec (85%) + Kaol	H20-4: Qtz		
	H17-18: Qtz + Kaol	H20-13: Qtz		
	H20-5: Rect + Ill/Smec			
	H20-7: Rect (13%)			
	H20-8: Rect (17%)			
	H20-9: Rect (18%)			
	H20-10: Rect (11%) > Kaol			

Table 3. X-ray diffraction data according to rock type and the presence or absence of fresh sanidine (intensity of alteration). Expansibilities, if calculable, are in parentheses.

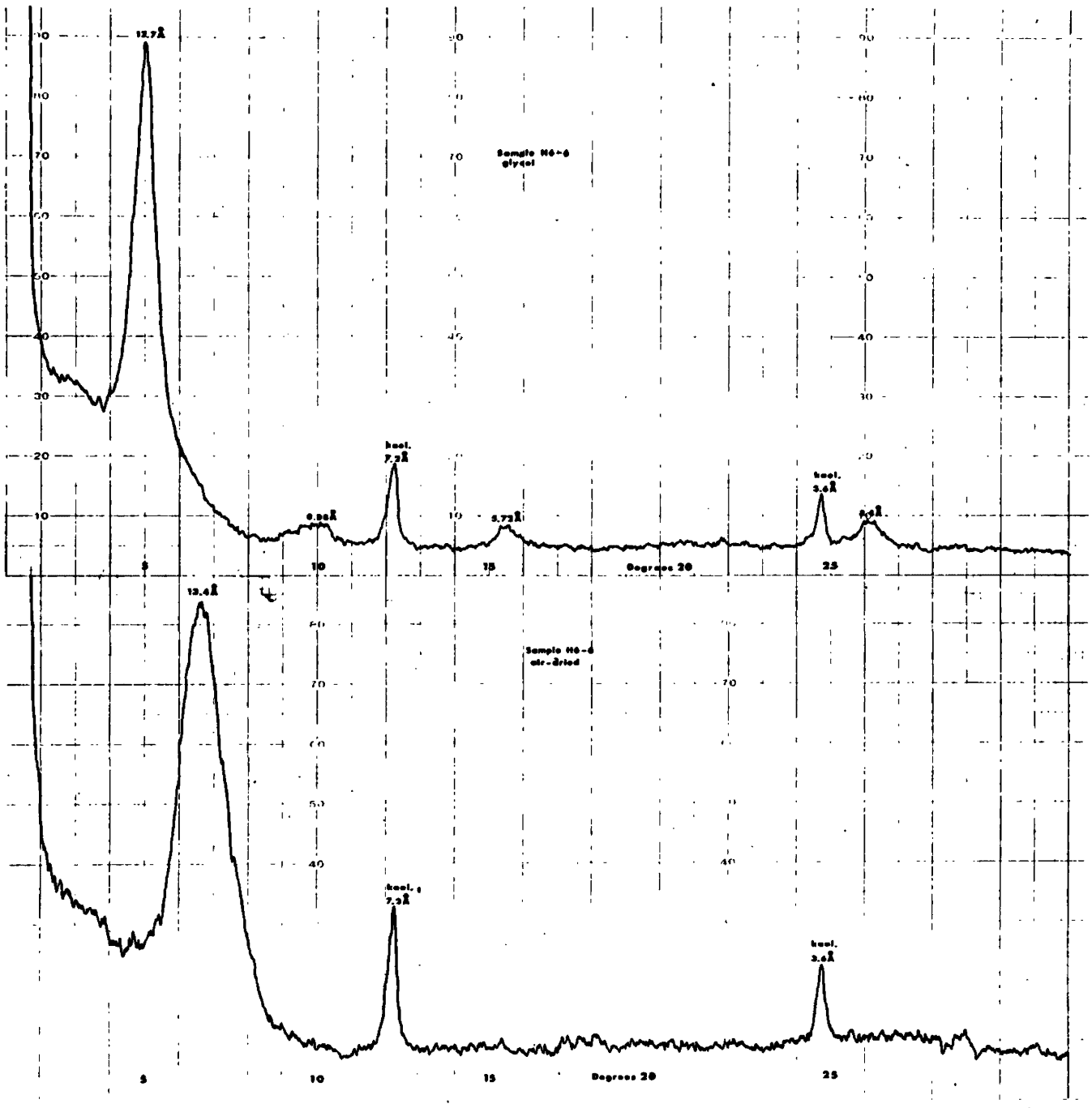


Fig. 6. X-ray diffraction patterns of air-dried and glycol treated smectite. Kaolinite is also present.

One randomly oriented sample (H6-6) has a peak at 1.49\AA indicating the smectite is dioctahedral (Eberl, 1978). This corresponds to montmorillonite or beidellite. The green color suggests nontronite, a beidellite in which ferric iron substitution for aluminum in the octahedral sheets is essentially complete. Chemical analysis is needed for reliable identification.

Illite/Smectite

Some of the clays are randomly interstratified mixed-layer illite/smectites. Their diffraction patterns also show expansion to a peak around 17.7\AA upon glycolation. They are distinguished from discrete smectite by variations in basal d-spacing reflections on the basis of methods of Sroden (1980) and Reynolds and Hower (1970).

Expansibilities were approximated using the combined 001/002 peak method of Reynolds and Hower (1970). Expansibilities ranged from 60-90% but may show over 30% error as discussed above. The return to near-background level reflections in the highly expansible ($\geq 80\%$) samples suggests that they may be discrete smectites as discussed above.

Rectorite

Occurring solely in the "potassic" rhyodacites with fresh sanidine is ordered mixed-layer illite/smectite. This is termed rectorite by Eberl (1978). Rectorite is distinguished by the presence of superlattice (combined mica-smectite) reflections in the low-angle 2θ region (fig. 7).

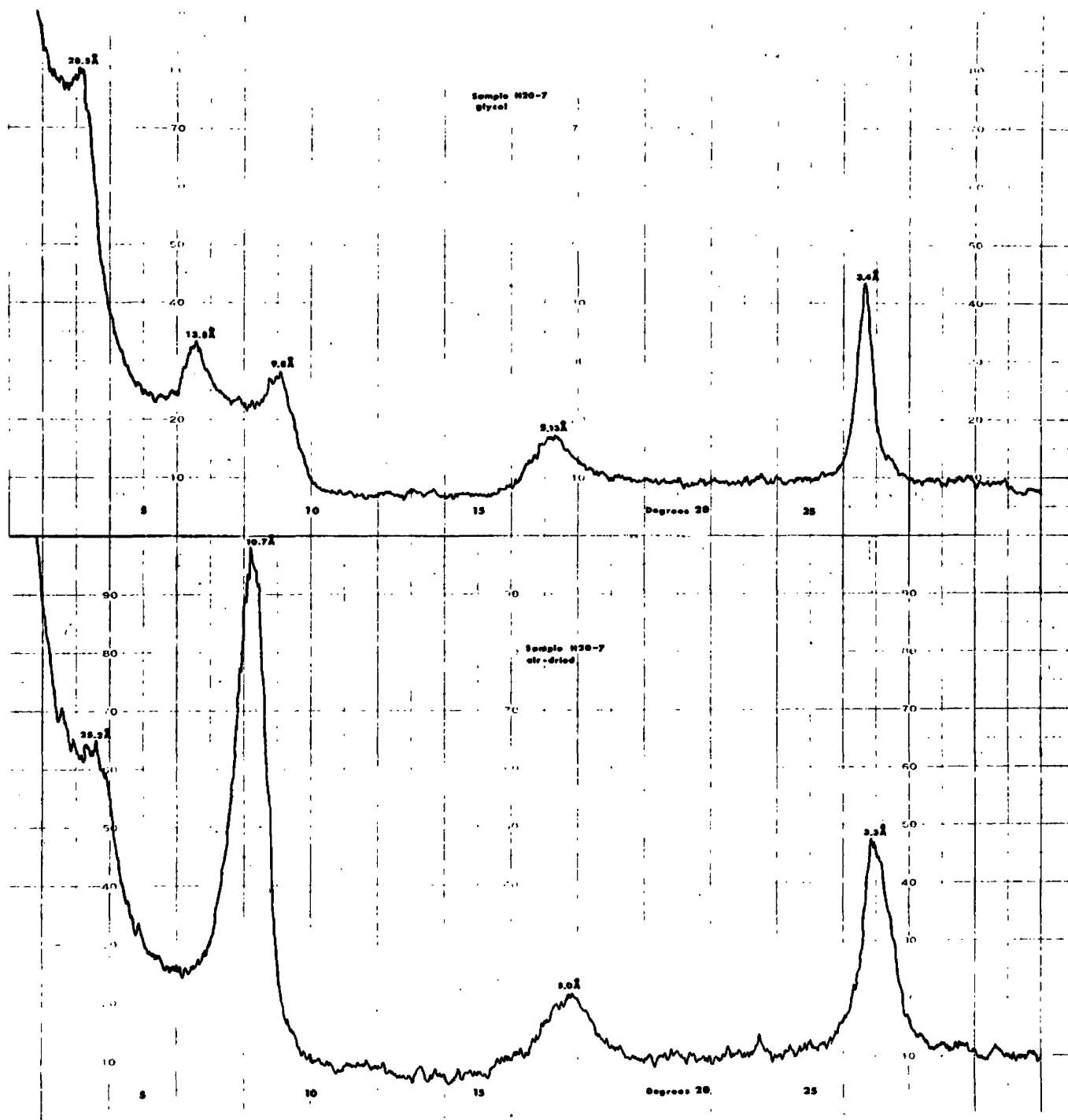


Fig. 7. X-ray diffraction patterns of air-dried and glycol treated rectorite.

A d-spacing around 25\AA (not always resolved) expands to $28\text{-}32\text{\AA}$ after glycolation. Deviation from an expected 27.6\AA peak (glycol) is attributed to the combined Lorentz-polarization factors (Stout and Jensen, 1968) in the low-angle 2θ region. In addition to the superlattice reflection, air-dried samples generally show peaks around 11\AA , 5\AA , and 3.3\AA . Upon glycolation peaks appear consistently around 13.5\AA , 9.8\AA , 5.2\AA , and 3.3\AA .

Percent expansibility was determined using the peaks in the vicinities of 15.5 and $26^\circ 2\theta$ (Sroden, 1980). Expansibilities ranged from 11-22%. All the rectorites have allevardite-like ordering, determined according to Sroden (1980) and Reynolds and Hower (1970).

Discrete Illite or Sericite

A few samples have a small but distinct 10.1\AA peak. This indicates a separate phase of illite or sericite.

Disordered Kaolinite

A kaolin group mineral is present in many "potassic"-rhyodacites and tuffs. It is the only clay mineral present where no fresh sanidine exists. Randomly oriented samples have a ramp or band head terminating at a d-spacing of 4.48\AA (fig. 8). This is characteristic of b-axis disordered kaolinite (Eberl and Hower, 1975). Halloysite can also have a band head over the same 2θ region. However, the sharpness of the peaks at 7.2\AA and 3.6\AA indicates the mineral is kaolinite. Halloysite has an extremely broad 002 peak and

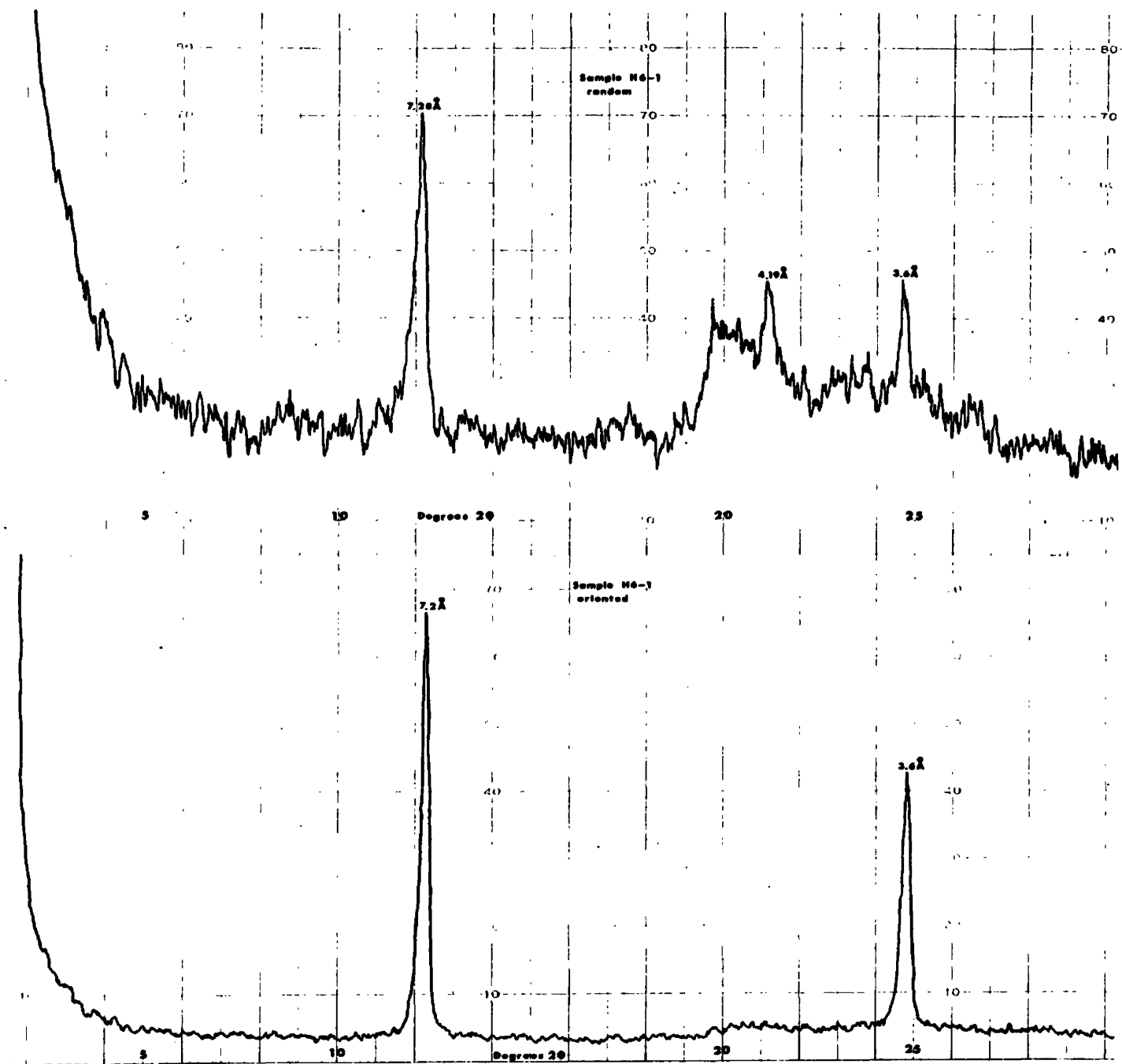


Fig. 8. X-ray diffraction patterns of oriented and randomly prepared b-axis disordered kaolinite.

is easily distinguished from kaolinite (Brindley and Robinson, 1948).

Quartz

Quartz is easily distinguished by peaks at 3.34\AA and 4.26\AA . It commonly crystallized larger than 2 micron size, though not exclusively. It was primarily recognized in randomly oriented samples.

Sulfates

Alunite $[\text{KAl}_3(\text{SO}_4)_2(\text{OH})_6]$ and jarosite $[\text{KFe}_3(\text{SO}_4)_2(\text{OH})_6]$ are present in a few samples, commonly associated with barite and sulfide minerals. Sulfide-rich samples from the dump (Main Level) have well-crystallized pink alunite replacing large feldspar phenocrysts. This alunite has a well-resolved diffraction pattern (fig. 9). Thin-section H17-14 has doubly terminating microlites that x-ray diffraction indicated were alunite and jarosite. Beudantite $[\text{PbFe}_3(\text{AsO}_4)(\text{SO}_4)(\text{OH})_6]$ may also be present, suggested by a 3.67\AA peak. Its other peaks are similar to jarosite peaks (3.08\AA , 5.94\AA , 2.54\AA , 2.29\AA) (JCPDS, 1980).

Kalinite. A white fibrous mineral growth occurs on much of the drill-core. It apparently had formed in storage over roughly a two year period. It appears to develop where mineralization is strongest. X-ray diffraction of randomly oriented samples indicates this mineral is kalinite $[\text{KAl}(\text{SO}_4)_2 \cdot \text{H}_2\text{O}]$ (JCPDS, 1980). It produced strong peaks at 4.83\AA , 4.33\AA and 3.47\AA with additional peaks at 3.99\AA , 3.80\AA ,

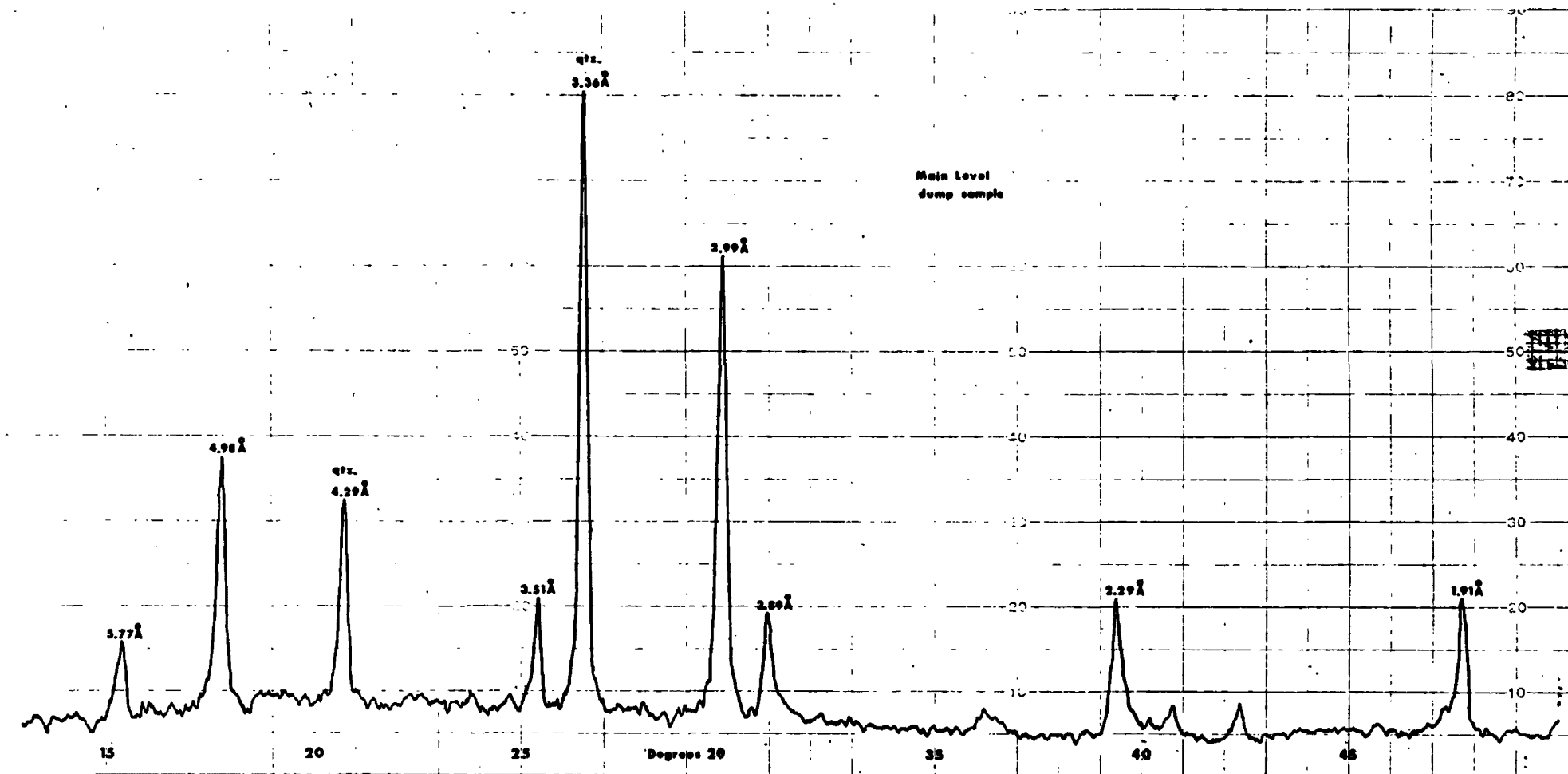


Fig. 9. X-ray diffraction pattern of alunite and quartz.

3.51Å, 3.3Å, 3.12Å, and 2.54Å.

Discussion

Secondary quartz is generally present, at least in small amounts, in all of the rocks. Much of the quartz resulted from the alteration of the silica-rich glass. Silicification and argillization may occur simultaneously (Hemley and Jones, 1964).

In a few samples, phenocryst alteration products differed from matrix constituents. X-ray analysis of the altered feldspar phenocrysts in sample H4-21 indicates disordered kaolinite. The x-ray pattern for the matrix in addition to the phenocrysts (<2 micron fraction) shows an addition of much quartz. The feldspars were argillized whereas the matrix was silicified. Some clay may exist in the matrix also, but its presence there was not proven. Similarly, in sample H2-9 the sodium cobaltinitrite-stained thin-section shows the potassium-bearing alteration mineral, rectorite, confined to altered feldspar phenocrysts whereas the groundmass is silicified. These samples indicate selective silica loss from the phenocrysts to the groundmass and aluminum retention in the phenocrysts.

In rocks with no fresh feldspar, both sanidine and plagioclase altered to b-axis disordered kaolinite. In rocks with some fresh feldspar, altered sanidine could not be distinguished from altered plagioclase. The prevalence of illite/smectites and smectite in many samples with dominantly fresh sanidine suggests that those clays replaced plagioclase.

clase. It is also likely that sanidine first altered to illite/smectite as discussed in chapter V.

Table 3 shows that the less intensely altered rocks are characterized by sanidine and expansible clays. Sanidine, randomly interstratified illite/smectite, and rectorite disappear with more intense alteration. Disordered kaolinite remains as the sole clay mineral. The transition boundary between the expansible-clay-sanidine assemblage and the kaolinite facies is sharp. The significance of this is discussed in chapter V.

Ore Mineralization

The high-grade ore described by Shenon and Taylor (1936) occurred as cellular deposits characterized by extreme silicification. The cellular structure developed as the soluble minerals were removed by leaching, resulting in numerous voids. The hypogene ore minerals, where they survived leaching, were galena, antimonial matildite (Ag-Bi sulfide) and lesser amounts of enargite. They commonly occupied former feldspar phenocryst sites. Supergene (secondary) minerals included argentite, covellite (rare) and marcasite (tentatively supergene). The principal gangue minerals reported were quartz, pyrite, barite, clays, alunite and jarosite. Oxidation products were common. The average silver grade for the first two years of production was 75 oz./ton.

The rich cellular ore described above was not encountered in this study. The mineralization found in the drill core

and on the surface essentially represents the low-grade fringe of the original ore body. Intensely silicified rocks with leached phenocryst voids are seen at the surface. Voids are filled with barite, pyrite and quartz or are vacant. Drill-holes intersect small silicified zones also, but rarely were any sulfides other than pyrite found filling feldspar molds. Remnants of the massive sulfide ore can still be found on mine dumps where marcasite, enargite and alunite are common.

The hypogene sulfides identified in this study by thin-section and polished-section analysis are pyrite, galena, sphalerite and a trace of chalcopyrite. Neither sphalerite nor chalcopyrite were reported in the cellular ores by Shenon and Taylor (1936). They may have been overlooked, but rapid spatial changes in ore mineralization are common in epithermal deposits. No secondary sulfide enrichment was recognized in this study.

Selected Metal Chemistry Discussion

Table 4 lists chemical analyses (see chapter III) for metals from drill-core samples. These values support previous data indicating that mineralization is accompanied by alteration and that the greatest metal values occur with the kaolinite facies alteration.

The richest sample analysed had 195 ppm silver (4.68 oz./ton). The silver content is generally sympathetic to the lead content suggesting the galena is argentiferous.

	<u>METALS</u>								
	"Sodic"- Rhy.	"Potassic"-Rhyodacites							Tuff
		Expansible-Clay Facies				Kaolinite Facies			
	<u>H2-1</u>	<u>H4-3</u>	<u>H20-8</u>	<u>H20-10</u>	<u>H4-16</u>	<u>H4-18</u>	<u>H20-12</u>	<u>H4-21</u>	<u>H17-23</u>
Bi	-	-	-	-	-	25	-	-	-
Ag	2.0	8.6	4.5	1.6	53	195	6.7	21	2.0
Cd	5	3	117	3	680	437	70	66	11
Co	10	12	17	14	16	16	19	15	18
Cu	12	24	15	17	118	191	66	20	38
Ni	12	19	14	10	12	39	12	80	21
Mo	6	10	18	14	66	22	12	6	14
Pb	432	272	860	155	5.93%	6.23%	2.58%	0.31%	630
Sb	11	11	10	9	16	22	11	11	11
V	74	109	101	127	167	61	107	81	83
Zn	525	303	1350	351	8.60%	4.76%	1.36%	1.32%	1800

NOTE: Values are in ppm unless marked by percentages.

Analyses performed by Technical Service Laboratories, Mississauga, Ontario.

Table 4. Metal chemistry of selected Flathead mine samples.

The silver in galena probably represents impurities such as admixed argentite or acanthite (Deer et al., 1966). Bismuth and antimony may indicate traces of silver sulfosalts. Chemical compositions of other minerals indicate that galena and sphalerite can account for the cadmium. Pyrite can contain cobalt, nickel, molybdenum and vanadium. Vanadium may also be present in magnetite, sericite and sphene (Deer et al., 1966).

Sample H2-1 ("sodic"-rhyodacite) contains small amounts of Ag, Pb and Zn, yet this unit is believed to post-date the ore-forming processes. Secondary dispersion (Levinson, 1974, p. 347-365) in the surface zone of oxidation and weathering probably accounts for this situation. This includes upward (capillary) or downward redistribution of metals by groundwater. Diffusion along elemental concentration gradients is common. Metals are easily adsorbed to clay mineral surfaces (Farah et al., 1980). Also, it is not unreasonable for rocks genetically related to ore-forming processes to be slightly enriched in those constituents.

Ore Control and Paragenesis

Evidence of mineralization controls and paragenesis is scarce and where present, often ambiguous. The low-grade ore in the rocks of the argillized fringe affords few samples with significant amounts of ore minerals. However, certain depositional aspects are apparent, primarily in polished-section study.

First, obliquely illuminated thin-sections reveal that mineralization was controlled by fractures and by porosity independent of fracturing. Sulfides and barite are commonly found in veins. Disseminated sulfides, except pyrite, are rarer. Galena is more regularly disseminated than sphalerite. In at least one sample (H4-18)(fig. 10), disseminated galena is localized around a central sphalerite and galena-bearing vein suggesting Pb migration away from that vein. In that same sample, pyrite is disseminated only in the wall-rock within and beyond the outer boundary of galena. The lack of pyrite in the vein suggests that it preceded the galena and sphalerite.

Open-space filling was the dominant manner of emplacement. Unfilled cavities are commonly found in the center of veins. Crustification textures (Park and MacDiarmid, 1975, p. 120-121) are evident. Sphalerite, with varying color due to varying iron content, forms bands along cavity walls with the center of the cavity unfilled. Also in sample H4-18 (fig. 11), sphalerite radiates outward from cavity walls with galena forming late as a "crust" on the sphalerite in the center. Unfilled spaces remain adjacent to the galena with some sphalerite crystals terminating in the cavity. An earlier generation of galena scattered along the cavity walls in the same sample, precedes sphalerite deposition.

Numerous fractures and leached phenocryst molds are only partially filled with singly terminating barite crystals.

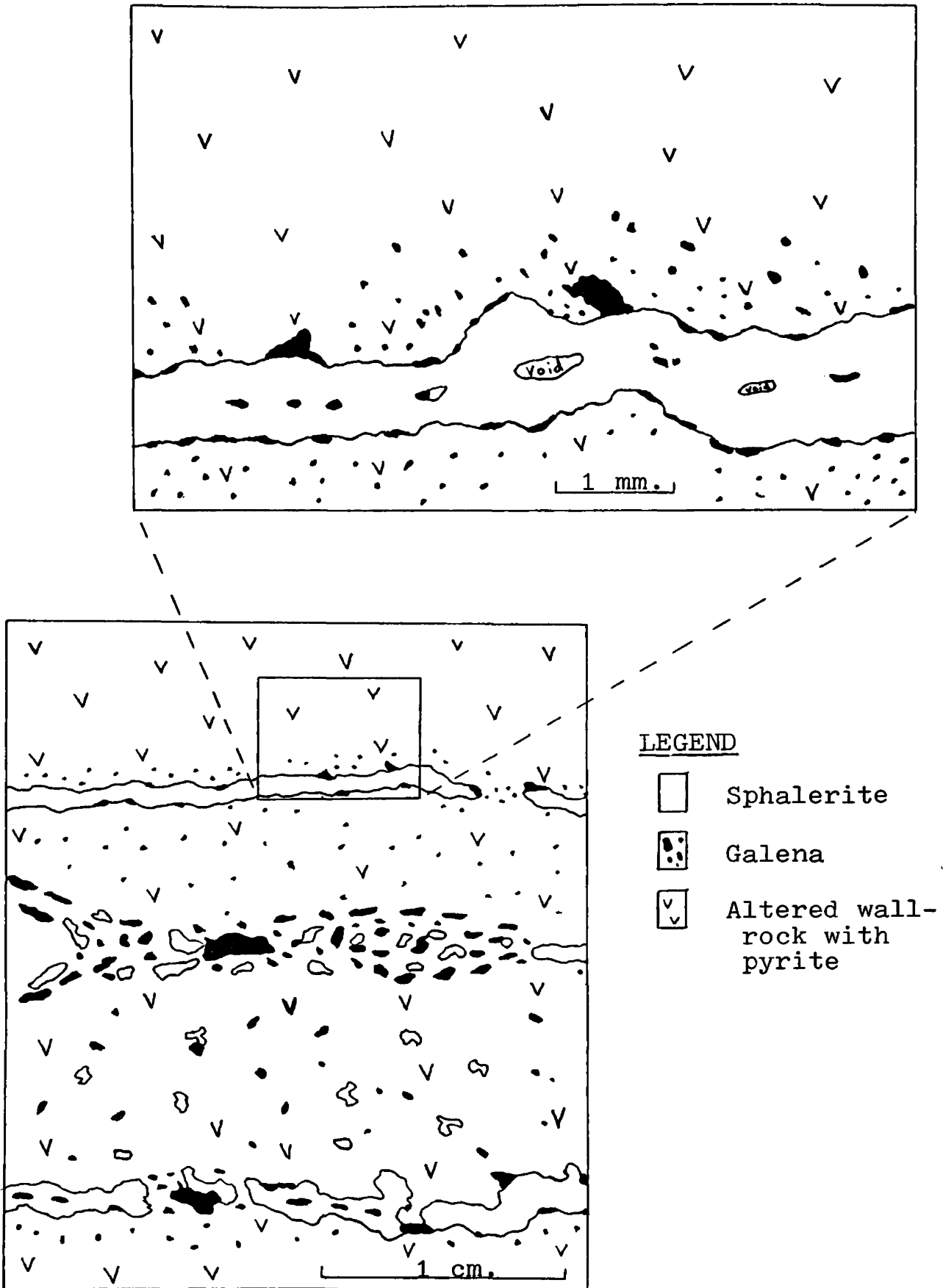
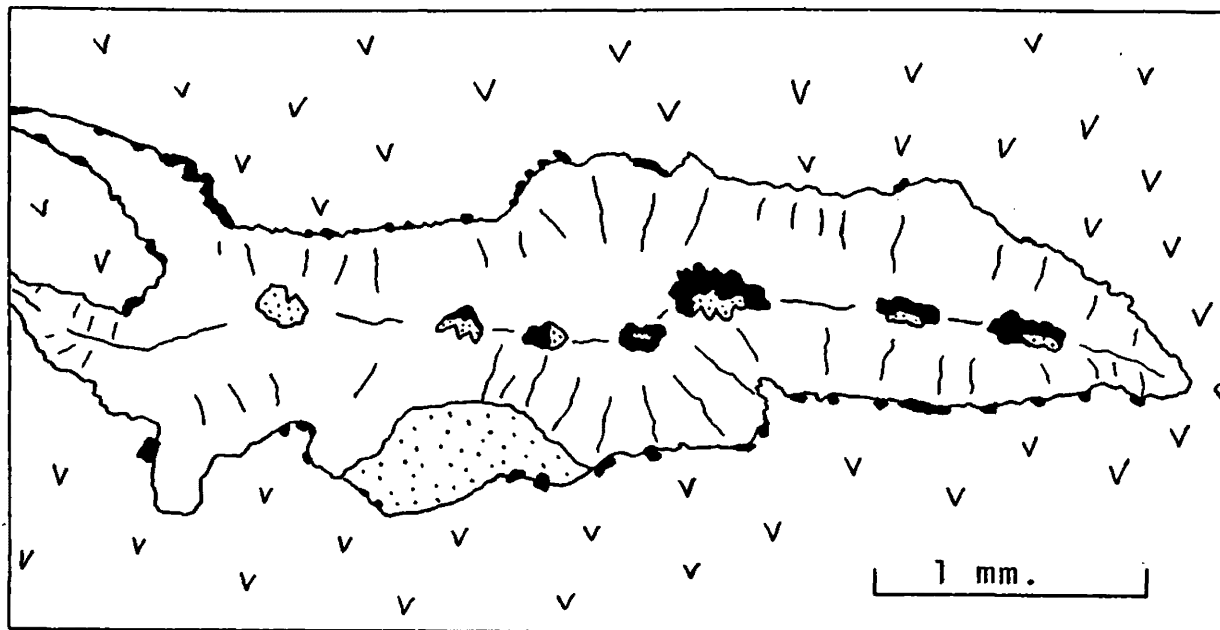


Fig. 10. Sphalerite-galena vein of sample H4-18 showing limited migration of Pb from the vein. Pyrite is disseminated in the wall-rock.



LEGEND

-  Sphalerite
-  Galena
-  Open space
-  Altered wall-rock

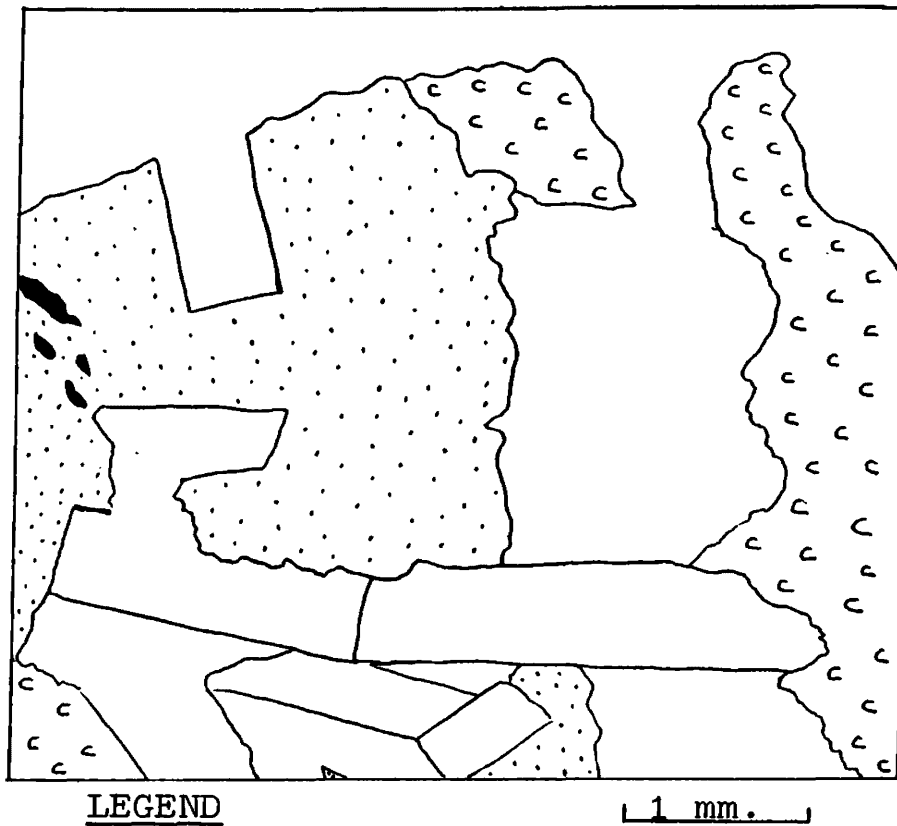
Fig. 11. Open-space fill texture of sample H4-18. Sphalerite radiates inward from the vein walls with a few crystals terminating in the central open cavities. Galena shows early and late generations.

In sample H20-12 (fig. 12) sphalerite is interstitial to euhedral barite, suggesting it was subsequent to barite deposition. Sample H17-11 has a brecciated fracture healed by open-space fill. Sample H6-14 shows well-developed crustification along cavity walls. Tridymite lines the walls, barite and olsacherite $[\text{Pb}(\text{SO}_4)(\text{SeO}_4)]$ coat the tridymite, and a late olsacherite vein cuts the tridymite and barite.

Olsacherite was identified by diffraction patterns (JCPDS, 1980) using an x-ray powder camera. Strong peaks occurred at 4.28\AA , 3.83\AA , 3.35\AA , 3.24\AA , 3.02\AA , 2.79\AA , 2.08\AA , and 2.04\AA .

Although open-space filling was the dominant mineralization process, some replacement also occurred. Whereas many veins are straight-walled, some sphalerite veins have convex edges suggesting replacement of wall-rock. Galena occupying portions of altered feldspar and amphibole phenocrysts may represent replacement. Sphalerite replaces biotite along cleavage planes in sample H2-12. Pyrite along phenocryst borders suggests replacement.

The evidence above concerning mineralization mechanisms also illustrates mineral paragenesis. Additional evidence includes galena coating barite in an open space (sample H2-18) and a pyrite vein being cut by a galena and sphalerite-bearing vein (sample H4-16). Small straight-walled veins alternating along strike between galena and sphalerite suggest an overlapping series of deposition. Pyrite crystals



LEGEND

1 mm.

-  Barite
-  Sphalerite
-  Clay
-  Galena

Fig. 12. Sphalerite growing interstitial to euhedral barite in sample H20-12.

imbedded in barite (sample H20-12) indicate contemporaneous deposition. Although voluminous amounts of data are lacking, the proposed paragenetic sequence is in figure 13.

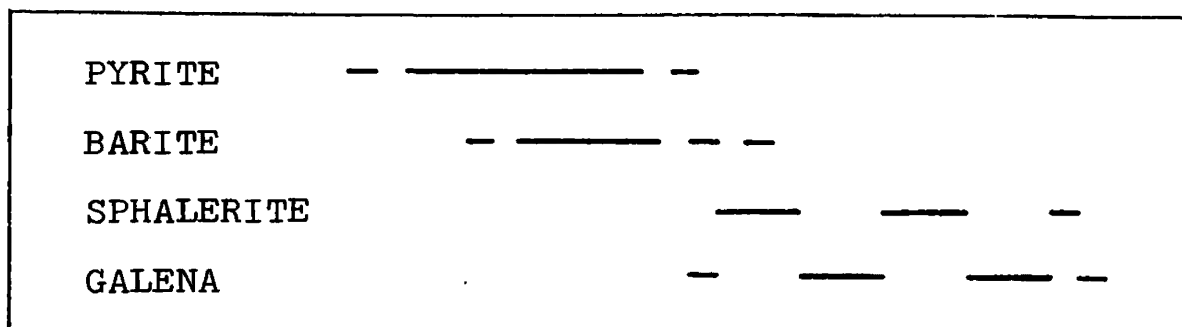


Fig. 13. Mineral paragenesis.

Depth of Formation

The open-space fill textures in these rocks indicate a shallow (low pressure) environment of formation. Shenon and Taylor (1936) concluded that the highest ridges in the area were never covered by volcanics so the difference in elevation between these and the Flathead ore body indicate a depth of formation less than 122 meters.

CHAPTER V
ALTERATION PROCESSES

The "potassic"-rhyodacite porphyry and rhyolite and rhyodacite tuffs at the Flathead mine are extensively altered. No fresh rock was found. Clay minerals and quartz are the major alteration minerals. Leucoxene and iron oxides are common in smaller amounts. Sericite, alunite, jarosite and carbonate are less common. The occurrence of alunite with sulfide-rich rocks suggests it was more common in the high-grade cellular ores previously mined out.

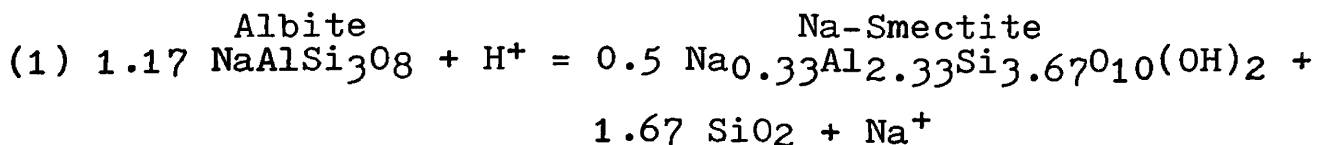
Argillic and silicic alteration assemblages dominate the mine area. Two distinct argillic facies are recognized and reflect different intensities of alteration. The less intensely altered assemblage is characterized by smectite, randomly interstratified illite/smectite, rectorite and the presence of fresh primary sanidine. The more intensely altered (i.e., advanced) assemblage is characterized by b-axis disordered kaolinite and the absence of fresh sanidine. Quartz is common in both assemblages.

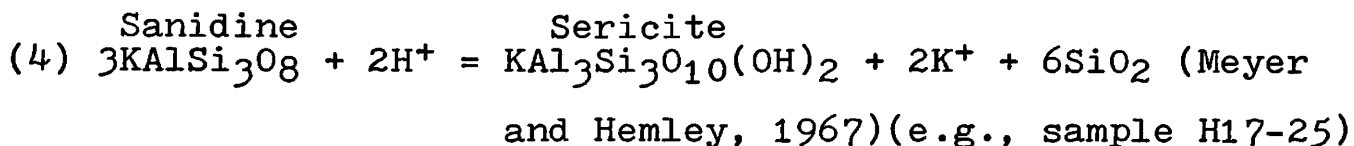
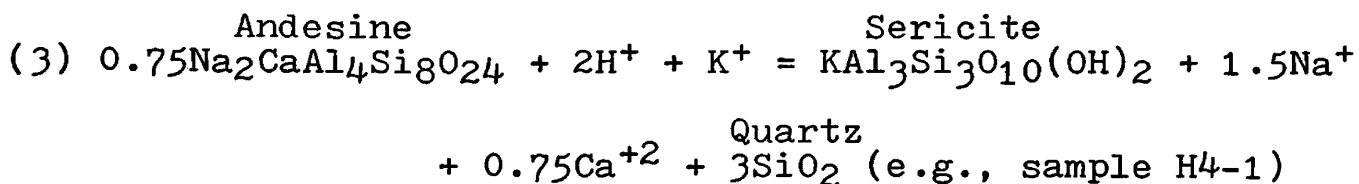
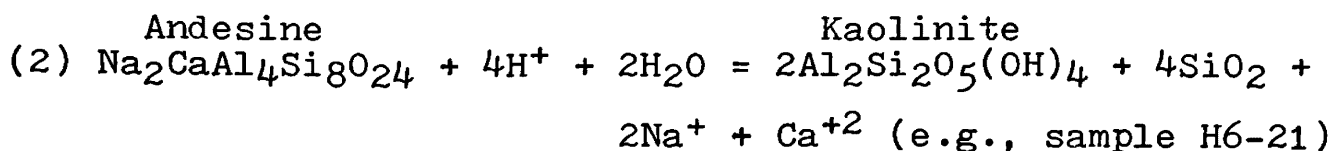
The formation of the alteration assemblages is best explained by the processes of hydrogen metasomatism (Hemley and Jones, 1964). Alteration results from chemical reactions

between rock minerals and hydrothermal solutions circulating through the rock. Silicate mineral instability can result from contact with acidic solutions that have low cation/H⁺ ion ratios. Chemical transfer occurs as H⁺ ions are added to the minerals. H⁺ ions combine with available oxygen atoms of the silicates to form the highly polarized hydroxyl groups of hydrous alteration minerals (Hemley and Jones, 1964). For every H⁺ ion introduced, a mole equivalent of base-metal cations is released to the solution, raising the cation/H⁺ ion ratio. As long as the cation/H⁺ ion ratio is low in the solution, hydrolysis reactions proceed. Mass transfer of chemical components was likely in the permeable units as solutions migrated through the rocks. Diffusion along concentration gradients contributes to transfer of chemical components in the less porous rock (Lovering, 1950).

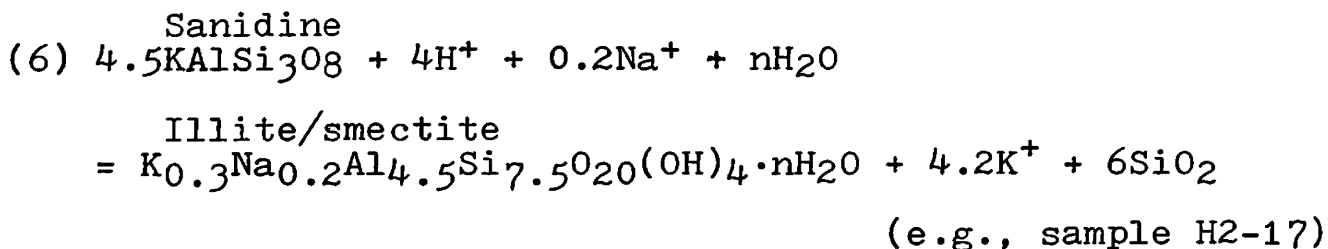
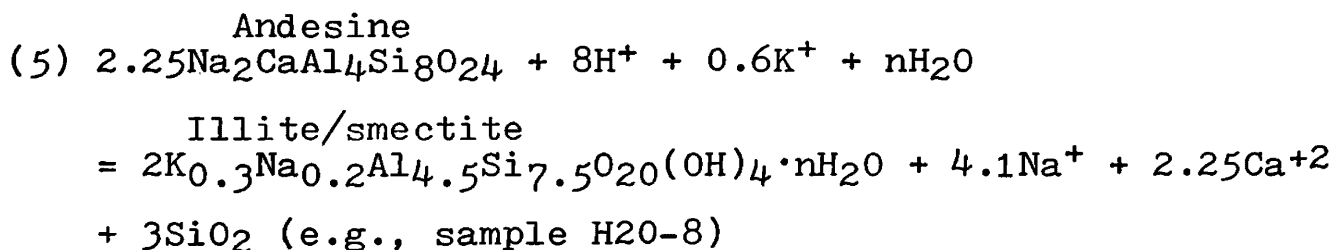
Expansible-Clay Facies

Whole-rock chemical values (table 1) illustrate the chemical leaching of the hydrothermal alteration process. Sodium was leached from the rocks in the expansible-clay facies as plagioclase replacement occurred. Sample H4-3 (1.18% Na) still has fresh plagioclase whereas sample H20-8 (0.23% Na) has none. Reactions associated with the chemical transfers of hydrogen metasomatism in this facies are listed below (Hemley and Jones, 1964):





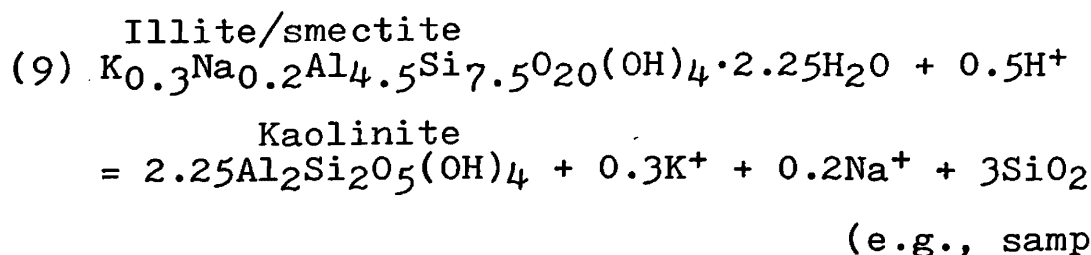
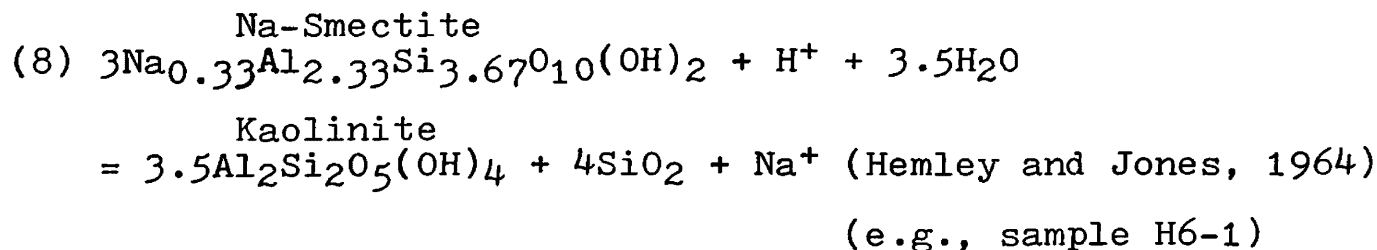
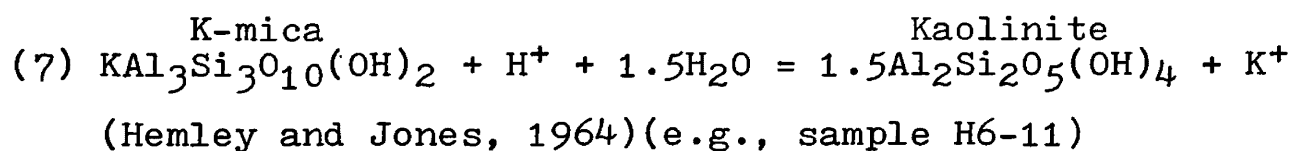
Kaolinite is present in the expansible-clay facies. Although sericite and discrete smectite are present only in small amounts, mixed-layer illite/smectites are common. The Flathead mine rocks are a combined Na-K system; mixed-layer illite/smectites could form as plagioclase and sanidine undergo alteration. Possible reactions are:



Mixed-layer illite/smectites can also form directly from smectite (Eberl, 1978). Sodium and calcium can serve interchangeably as interlayer cations in the expansible clays.

Kaolinite Facies

Variation diagrams (fig. 14a. & b.) illustrate the chemical differences between the expansible-clay facies and the kaolinite facies. The rocks of the kaolinite facies are thoroughly depleted in calcium, magnesium, sodium and potassium compared to less depletion in the expansible-clay facies. Sanidine is destroyed in the kaolinite facies. As long as sanidine was present (expansible-clay facies) altering solutions remained sufficiently rich in potassium for the stabilization of K-micas and mixed-layer illite/smectites. With the disappearance of sanidine, altering solutions no longer had a source for potassium, rendering the K-micas and K-clays unstable. Leaching of silicon, calcium magnesium and sodium destabilized smectite as well as mixed-layer illite/smectites producing b-axis disordered kaolinite. Possible reactions depicting these changes are:



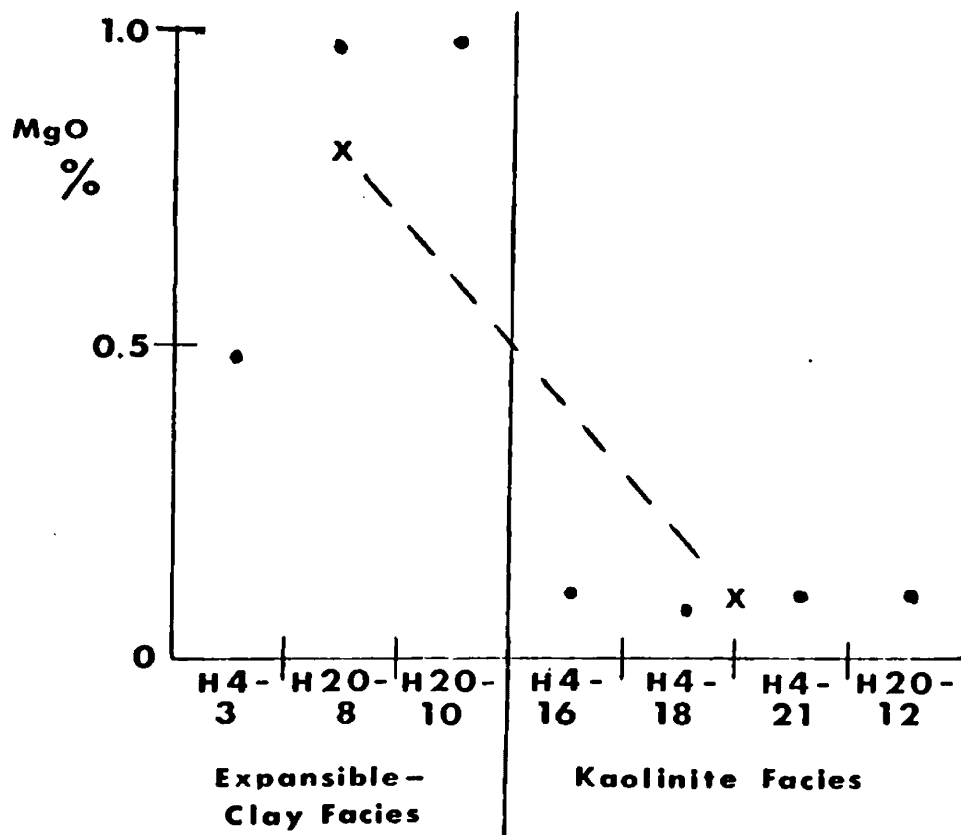
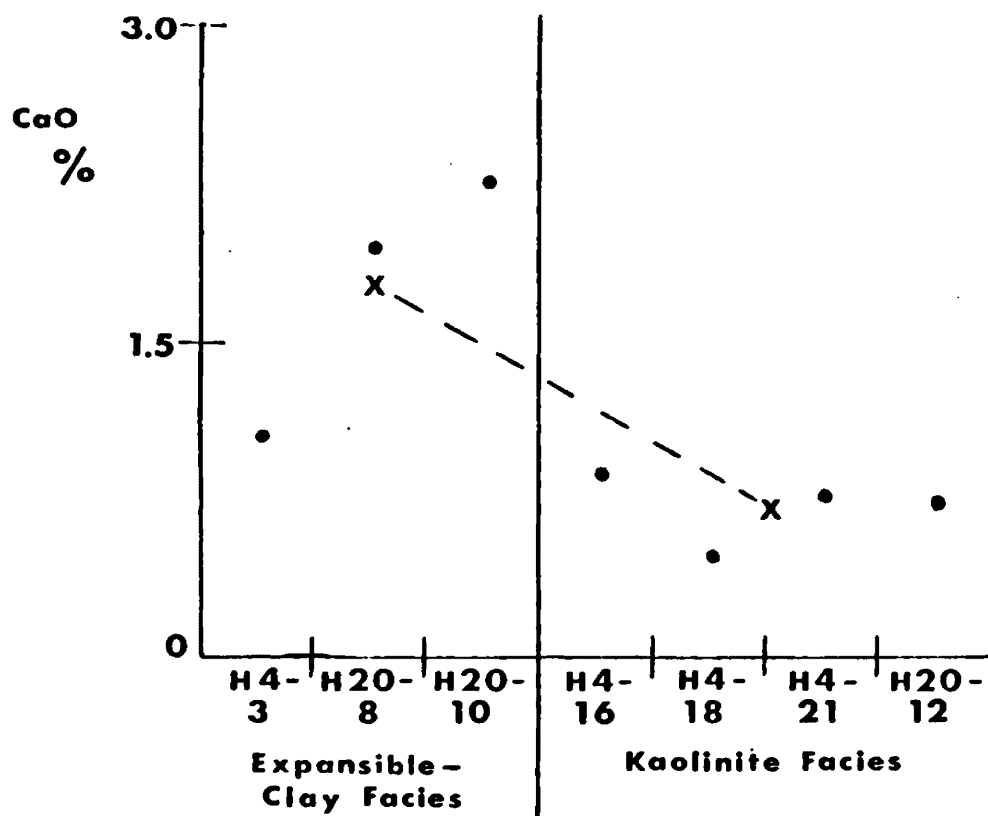


Fig. 14a. Variation diagrams illustrating the depletion of Ca and Mg in the kaolinite facies with respect to the expansible-clay facies. X's represent the average chemical percentage for each facies. Dashed line indicates the difference between the average values.

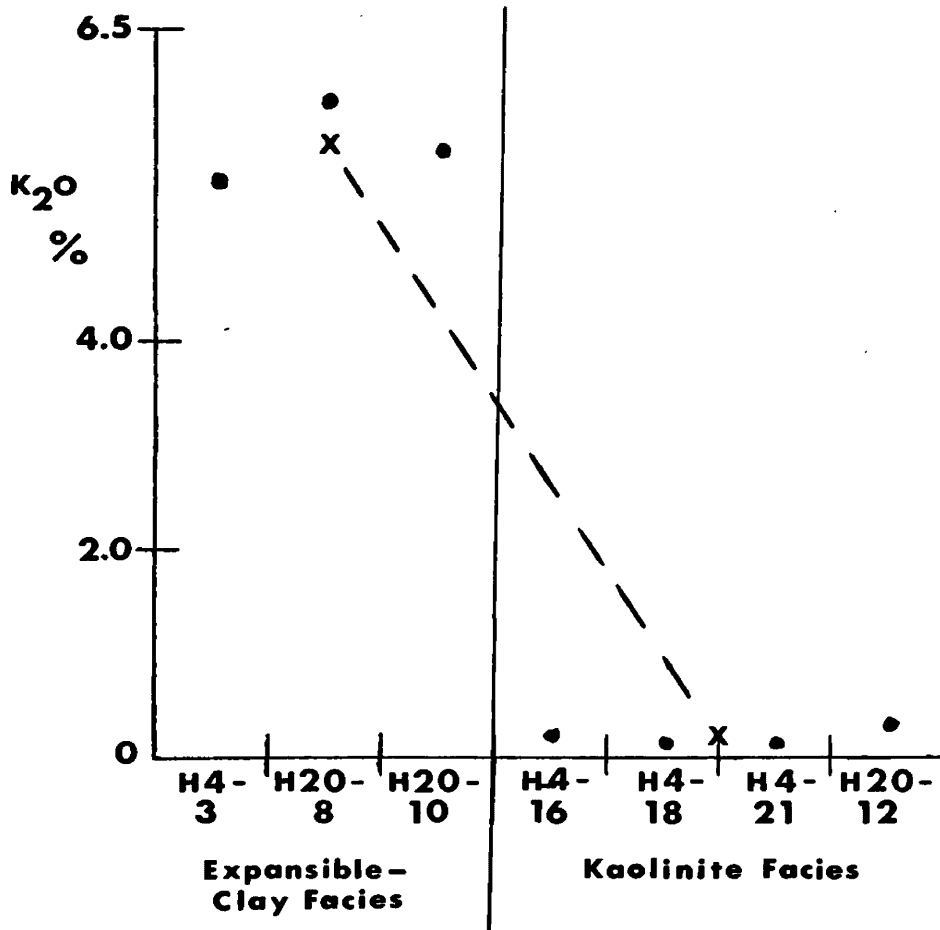
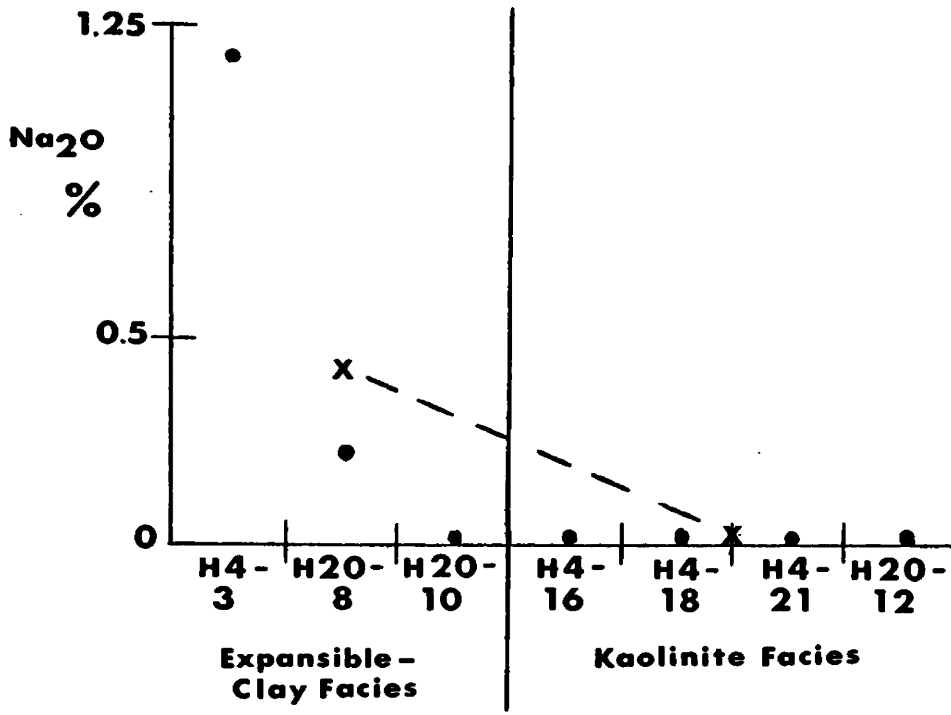


Fig. 14b. Variation diagrams illustrating the depletion of Na and K in the kaolinite facies with respect to the expansible-clay facies. X's represent the average chemical percentage for each facies. Dashed line indicates the difference between the average values.

Equations similar to (8) and (9) can be written for clays with calcium.

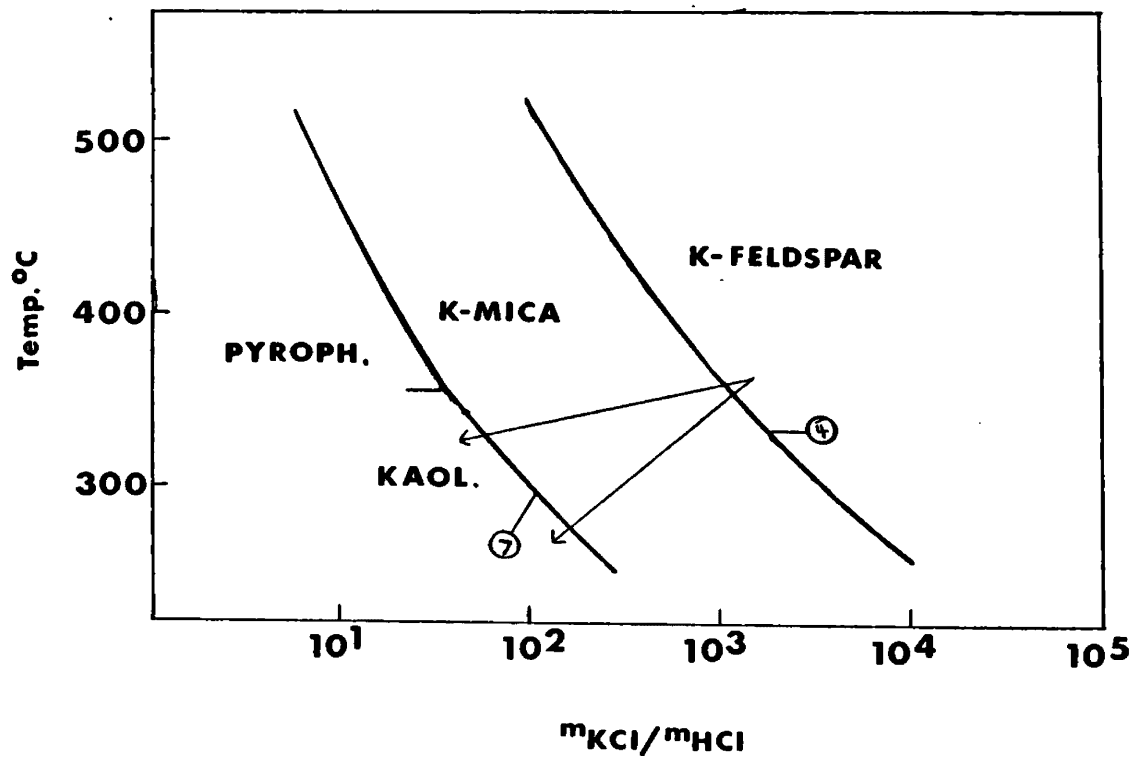
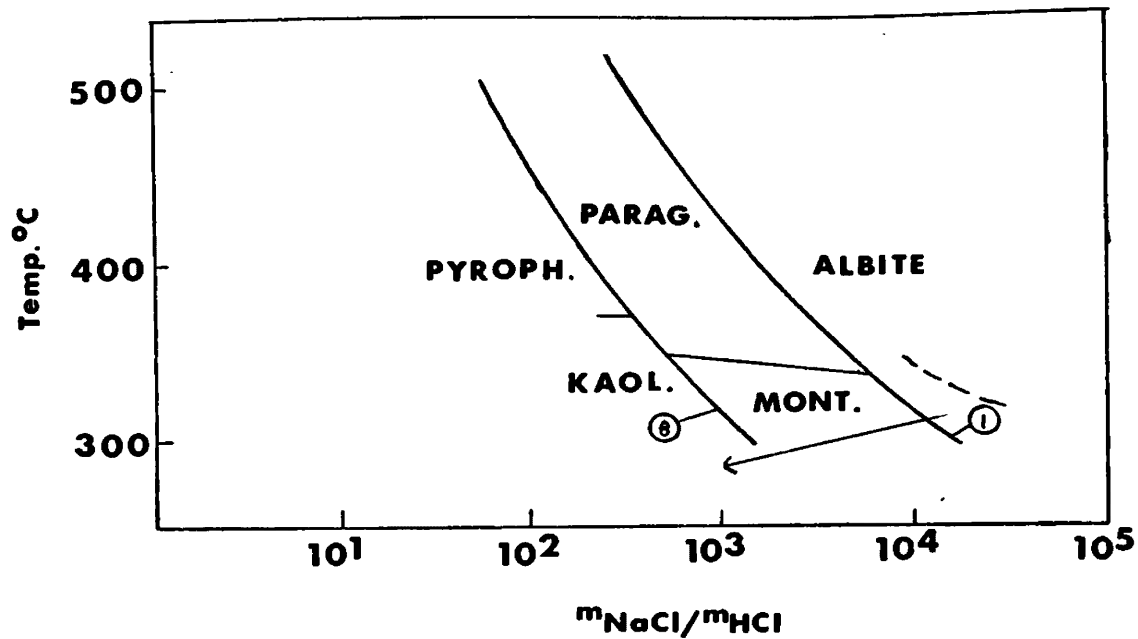
Silicification

It is apparent from the reactions above that silicification may accompany argillization without an influx of silica [e.g., eqs. (2) and (6)]. However, in places silicification appears to result from an addition of silica (e.g., sample H20-1). The diminished density of these rocks, due to acid leaching, is not sufficient to account for the increased percentage of quartz. The silica was probably derived from the hydrolysis of silicates in the argillized rocks. Solutions with high silica activity moved to areas of high H^+ activity. This high H^+ activity caused the silica to reprecipitate (Meyer and Hemley, 1967). Extreme silicification leaves rocks composed of little else but quartz. This is the most advanced alteration type at the Flathead mine. Molds from leached phenocrysts are common in these rocks. They are filled with barite and pyrite or are vacant.

Equilibrium Diagrams

The mineralogic changes and chemical reactions characteristic of the argillic alteration at the Flathead mine described above are illustrated on equilibrium diagrams with hydrolysis reaction curves (figs. 15 & 16). These diagrams illustrate the effects of changing temperatures and cation/ H^+ ion ratios in the altering solutions.

The equilibrium diagrams of fig. 15 would apply rigorously



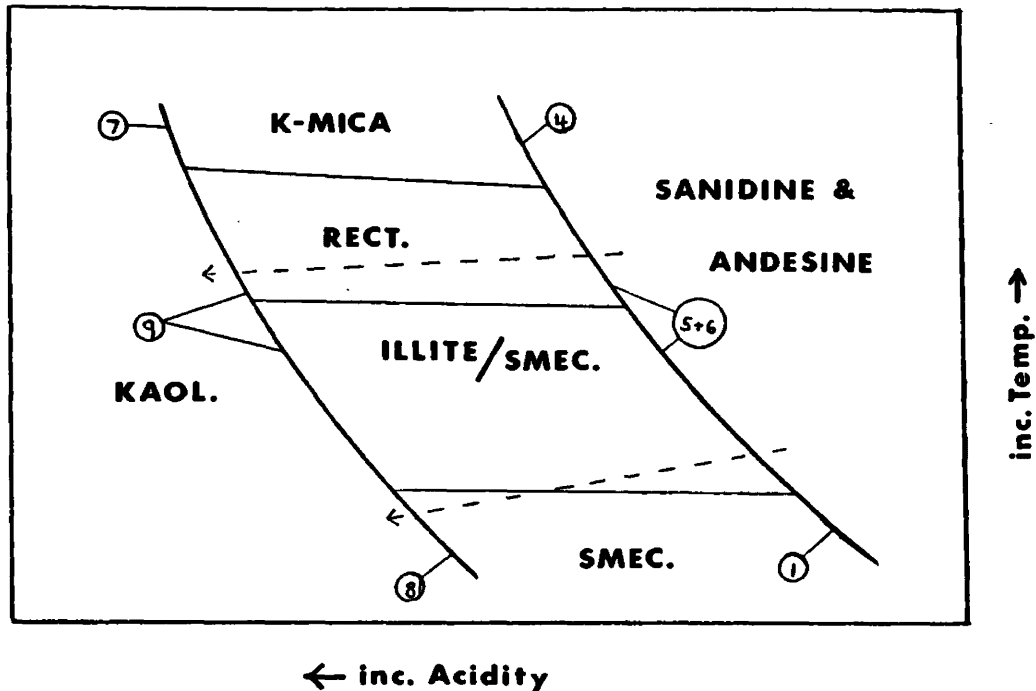


Fig. 16. Hypothetical equilibrium diagram (qualitative) representing the combined Na and K systems of fig. 15. Andesine contains some calcium. Dashed arrows represent possible paths of the alteration fluids (different temps.) at the Flathead mine. Circled numbers relate reaction curves to equations in the text.

Fig. 15. Reaction curves for the system $\text{Na}_2\text{O}-\text{Al}_2\text{O}_3-\text{SiO}_2-\text{H}_2\text{O}$ (top) and the system $\text{K}_2\text{O}-\text{Al}_2\text{O}_3-\text{SiO}_2-\text{H}_2\text{O}$ (bottom) at 15000 psi total pressure with quartz present. Dashed line in top diagram is a segment of the decomposition curve of anorthite to Ca-mont. in CaCl solutions (Meyer and Hemley, 1967). Solid arrows represent possible paths of the alteration fluids at the Flathead mine. Circled numbers relate curves to equations in the text. From Hemley and Jones (1964).

only to the alteration of rocks consisting exclusively of K-feldspar or plagioclase and quartz. Fig. 16 is a qualitative representation of a combined K-feldspar/plagioclase system. The hydrolysis reaction curves were not experimentally derived. The slopes of the reaction curves mimic those of fig. 15. Fig. 16 illustrates more closely the proposed course of alteration at the Flathead mine.

The presence of kaolinite and quartz in the argillized rocks at the Flathead mine is noteworthy with respect to temperatures of alteration. Kaolinite plus quartz thermally decompose to form pyrophyllite (fig. 15). No pyrophyllite is found, thus an upper temperature limit of about 400° C is imposed on kaolinite and quartz-bearing assemblages (Hemley and Jones, 1964). The 400° C limit is subject to change with the increasing complexity (i.e., additional components) of natural systems.

Between the hydrolysis reaction curves in fig. 16 are the alteration minerals found in the expansible-clay facies at the Flathead mine. Reaction series of the kind illustrated were derived experimentally (Eberl, 1978) and are found in natural systems (Hower et al., 1976; Muffler and White, 1969). Depending on composition, smectites can survive up to 450° C at low pressures (Meyer and Hemley, 1967). However, with abundant K^{+} ions, smectites can thermally transform to mixed-layer clays and eventually discrete illite. K^{+} ions are supplied by the gradual breakdown of

sanidine. Temperature and reaction times are the main factors controlling the extent of conversion (Hower et al., 1976). Complete conversion of mixed-layer clays to discrete illite takes place around 200° C (> 175° C - Hower et al., 1976; < 210° C - Muffler and White, 1969). The particular clay minerals of the expansible-clay facies may reflect paleo-temperatures. The rarity of K-mica in the expansible-clay facies suggests that temperatures may never have exceeded 200° C.

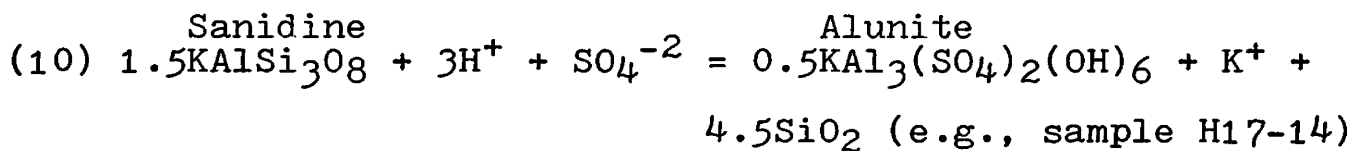
The hydrolysis reaction curves (fig. 15) were calculated for higher pressures than probably existed at the Flathead mine. However, they are qualitatively illustrative. A decrease in pressure would tend to shift the hydrolysis reaction curves to the left.

Anionic Metasomatism

Other alteration products occur at the Flathead mine as a result of anionic metasomatism. CO_3^{-2} metasomatism produced a carbonate mineral replacing feldspar. Sample H20-8 has an anomalously high value for manganese, but also significant calcium. This mineral could be either rhodochrosite or calcite, or a solid solution of the two (Palache et al., 1951). It occurs predominantly in the expansible-clay facies, but carbonate development may not be contemporaneous with clay formation. Carbon dioxide and water react to product carbonic acid only in alkaline solutions; carbonate minerals form only in alkaline environments as at Cochiti,

New Mexico (Bundy, 1958) and Summitville, Colorado (Steven and Ratté, 1960).

A more advanced form of anionic metasomatism, with the addition of SO_4^{-2} , produces alunite and jarosite in the extremely silicified rocks and the kaolinite facies. These minerals commonly occur with concentrations of barite and sulfide minerals. Alunite replaces sanidine phenocrysts at the Flathead mine and can alter directly from it or replace sericite that previously replaced the feldspar (Schwartz, 1955). Possible reactions are:



The most likely environment of formation for sulfates is near the surface within the zone of meteoric water circulation and oxidation. The oxidation of H_2S and pyrite produces sulfuric acid. Limonite and hematite testify to oxidizing conditions. These supergene solutions have low cation/ H^+ ion ratios. Alunite is typical of acid hot-springs environments (White, 1955).

Discussion

Hydrothermal solutions must be acidic for hydrogen metasomatism to occur. The solutions may evolve internally to acquire their base-leaching capacity (Meyer and Hemley, 1967). This could happen with: 1) an influx of juvenile

gases and acid vapors; 2) oxidation (e.g., $\text{H}_2\text{S} + 2\text{O}_2 = \text{H}_2\text{SO}_4$); 3) decreasing temperature which progressively dissociates acids (e.g., $\text{HCl} = \text{H}^+ + \text{Cl}^-$); 4) the pyritization of mafics by H_2S or HS^- ; and 5) the precipitation of sulfides (e.g., $\text{metal} + \text{H}_2\text{S} = \text{sulfide} + 2\text{H}^+$) (Meyer and Hemley, 1967).

The more advanced alteration assemblages "overprint" the less intensely altered rocks as solutions become more acidic by processes described above or as the buffering capacity of the rocks is gradually overcome.

The kaolinite facies is a more advanced type of alteration than the expansible-clay facies. Cation leaching occurred to a greater extent (fig. 14a. & b.). Extreme silicification characterized by the absence of clays is the most advanced type of alteration at the Flathead mine. Cation exchange and leaching are the dominant activities of the hydrothermal solutions in wall-rock alteration. They can result in increased porosity and permeability for the host rocks, especially characteristic of advanced silicification (Lovering, 1950). In the Flathead mine ore body the most advanced alteration is associated with the greatest metal concentrations.

Extensive leaching in the extremely silicified porphyry rocks probably provided openings (e.g., feldspar molds) for mineral deposition. It is also probable, therefore, that leaching and silicification preceded mineralization in the

rich cellular ores previously mined out.

Argillization did not create the numerous open spaces characteristic of the intensely silicified rocks. Openings for mineralization are largely provided by fractures in argillized rocks. The kaolinite facies, more sulfide-rich than the expansible-clay facies, probably originated as a result of mineralization. Sulfide precipitation lowers the pH of solutions locally, resulting in increased hydrogen metasomatism. These solutions are then buffered by reactions with the wall-rock farther from depositional sites.

The boundary between the expansible-clay facies and the kaolinite facies is sharp. No expansible clays survive in the absence of sanidine. However, sanidine destruction within the expansible-clay facies is gradual. Kaolinite exists in the expansible-clay facies also, probably by destruction of plagioclase (eq. 2) or smectite (eq. 8). Potassic minerals require more acidic solutions to convert to kaolinite.

The large-scale alteration "package" at the Flathead mine occurs in no simple geometric pattern either laterally or vertically (fig. 4a. & b.). The former rich core was extremely silicified (Shenon and Taylor, 1936) and is non-symmetrically surrounded by two distinct argillic facies. This is attributed to differential fracturing and thus variable permeability of the wall-rocks. Maximum interaction between wall-rocks and hydrothermal solutions, and thus more

advanced alteration, occurred where permeability was greatest. However, it is likely that the more advanced argillic assemblage (kaolinite facies) borders the core (i.e., extremely silicified rocks, especially where mineralized) as in fig. 4a. & b. though expansible-clay facies alteration borders extreme silicification at the surface near drill-hole H4 in the Lead Pit (fig. 2).

CHAPTER VI
THE VOLCANIC ENVIRONMENT

Evidence presented indicates that a hydrothermal convective cell (i.e., hot-springs system) existed at the Flathead mine. Hydrothermal alteration characterized by kaolinite, reprecipitated silica and alunite implies an acid hot-springs origin (Lovering, 1950; White, 1955). A hydrothermal convective cell of recirculated water would account for the formation of alunite at deeper levels (Main Level) in the deposit (White, 1955). The open-space fill textures of hypogene minerals indicate shallow depths of deposition.

Evidence suggesting that the Flathead mine ore body occurs at or near an ancient volcanic vent includes: 1) a thick volcanic pile (drill-holes nowhere reached Belt rock whereas Belt rocks outcrop less than one kilometer east and west of the mine); 2) intrusive rocks at depth that are coequal (i.e., "potassic"-rhyodacites) with extrusive flows (Johns et al., 1963); 3) ancient fumarolic deposits near the Ole mine (fumaroles are common near vent areas); 4) fractures - logical associates of vent eruptions; and 5) hot-springs type mineralization and alteration; hot-springs are characteristic of the end-stage of volcanic activity in vent

areas (Smith and Bailey, 1968).

The "sodic"-rhyodacite porphyry caps the altered rocks at the Flathead mine. These rocks show no unequivocal hydrothermal alteration and rocks of this type do not occur at depth at the Flathead mine. This suggests they did not originate from the proposed vent at the Flathead mine.

Precipitation of the Ore

Ore precipitation probably resulted largely from the mixing of meteoric water with metal-bearing solutions within the convective hydrothermal cell. A complete description of ore-precipitating mechanisms depends on whether metals were transported by chloride or sulfide complexes. In either case, dilution by meteoric water would decrease the concentration of the complexing ion (Cl^- , S^{-2}) and reduce the temperature of the solution resulting in decreased metal solubility (Barnes, 1979). The association of ore minerals with sulfate minerals (barite and alunite) may not be coincidental. Sulfate reduction increases H_2S concentrations and causes sulfide precipitation from chloride complexes (Barnes, 1979). Sulfide complexes are oxidized where mixed with oxygenated meteoric waters but exposure to oxidized minerals such as sulfates also causes oxidation of sulfide complexes. The sulfide concentration is lowered by oxidation of sulfide, resulting in precipitation of the complexed metals. Oxidation generates H^+ ions to the extent that the sulfide is protonated, if at all, which decreases the pH of

the solution and the activity of the complex-forming species thus decreasing metal solubility (Barnes and Czamanske, 1967).

In sample H20-12, small pyrite crystals are imbedded in barite. Barite and pyrite can crystallize together in equilibrium (Barnes and Czamanske, 1967). However, this texture may indicate mixing of sulfide and sulfate-bearing solutions with subsequent rapid deposition before solutions could equilibrate. In the Kuroko deposits of Japan, ore solutions were rapidly cooled and supplied with sulfate ions upon mixing with seawater (Urabe, 1978). This led to simultaneous deposition of sulfides and sulfates. Similar precipitation could have occurred at the Flathead mine by the mixing of hot ascending reduced ore-bearing solutions with cooler descending oxidizing meteoric water in a hot-springs environment. Many rocks have ore minerals confined to veins. This suggests rapid precipitation, not permitting migration away from the vein (Meyer and Hemley, 1967). Rapid precipitation indicates rapid chemical and/or physical changes in the solution such as rapid cooling that could result in the mixing of sulfide and sulfate solutions.

Throttling could cause deposition along narrow fractures, and precipitation by adiabatic expansion could have occurred if fractures were open to the surface. The argillized rocks may have enclosed the high-grade core in a relatively impermeable shell, except where fractures existed, since argillization may reduce permeability (Park and MacDiarmid, 1975, p. 138).

CHAPTER VII

VOLCANIC SILVER DEPOSITS: A COMPARISON

Ore-grade concentrations of silver are found in the circum-Pacific zone of Tertiary volcanism. The deposits are generated above subduction zones at convergent plate boundaries (Sillitoe, 1977) and are associated with intermediate to silicic volcanic host rocks.

The Flathead mine volcanics probably originated in such a fashion. The Tertiary subduction zone was generally located along the northwest Idaho border until the mid-Oligocene when it moved to its present west coast location (Alt and Hyndman, 1978). Magmas related to subduction can apparently occur far inland of trench-arc boundaries because of rapid subduction rates (Coney and Reynolds, 1977). The deposits in Nevada and Colorado are far inland of subduction zones.

Features of 12 major tertiary epithermal silver deposits and the Flathead mine are listed in table 5. In these deposits, structural features largely control the occurrence of alteration and mineralization. Fractures and fissures provide channelways for the hydrothermal solutions and openings for mineral deposition. Textures indicate that

DISTRICT	VOLCANIC ROCKS	ORE CONTROL	MAJOR ALTERATION	MINERALIZATION	GANGUE	PARAGENESIS	SUPERGENE MINERALS
Bonanza, Colorado (11)	andesite latite rhyolite = poor ore	fault-fissures o.s.f. w/rep.	Sil (qtz, chal, alun, kaol, py) Ser (py, qtz, carb, rut) Prop (chl, cal, qtz, ep, ser, rut)	py, sp, gn, cp, bn, ten, strom, en, chal, pyra, prou, Ag+Au tellurides	qtz, cal, bar, flu, ad, rhodc	1) Sil 2) ser, py, bar, sp, qtz 3) bn, en, gn, cp, ten, chal, strom	native Ag
Cochiti, New Mexico (10)	andesite	rep. o.s.f.	Dickite (qtz, py) Ill-Kaol (leux, jar) Verm-Halloy (allo, jar, leux, alun) Prop (chl, mont, ep, mag, cal, leux) Silicification	arg, sp, cp, gn, Au, py	qtz, py, cal	1) cal 2) qtz 3) py 4) cp 5) sp 6) gn 7) qtz 8) py 9) arg	goethite, gypsum, melanterite, lepidocrocite
Comstock Lode, Nevada	andesite rhyolite (18)	faults fissures (18)	Silicification Sericitization Prop (ep, chl, albite, cal, mag, clinoz) Zeolitic (albite, py, cal, natrolite) (12)	py, Au, Ag, elect, sp, gn, arg, cp, poly, stephanite (5,18)	qtz, cal, py, ankerite? (5,18)	1) qtz, sp 2) cp, gn, arg (5)	covellite, chal, poly, native Ag, arg, angle-site (5)
Flathead Mine, Montana	rhyodacite rhyolite	fractures o.s.f. w/ some rep.	Silicification w/Qtz, alun, py, jar Kaol (Qtz, py, leux, alun, jar, hem) Rect-Ill/smec (Qtz, py, smec, kaol, leux, hem) Carbonatization	gn, antimonial matil-dite, en, sp, cp	qtz, bar, py, clays, alun, oxides	1) Silicification, Expansible-clay facies, py 2) barite 3) gn 4) sp 5) gn 6) Kaol. facies	arg, cov, marc
Goldfield, Nevada	andesite latite rhyolite dacite = best ore	fissures caldera o.s.f. rep.	Alun-Qtz (hem, jar, ep, rut, gyp, pyrophyllite) Ill-Kaol (Opal, ad) Mont (ilmenite) Argillized zones w/halloy, hem, leux, jar, gyp Prop (chl, verm, cal, antigorite) (22)	py, sp, wurtzite, ten, famatinite, bismuthinite, sylvanite petzite, hessite, Au, goldfieldite (59)	qtz, chal, alun, kaol, ep, zircon, marc (59)	alteration first 1) ten, fam, sp 2) bis 3) goldfieldite 4) Au, Ag (59)	jar, gyp native Au (44)
Guana juato, Mexico (40)	rhyolite andesite	veins + stockwork faults (20)	adularia	acan, poly, pyra, cp, sp, gn, Ag, Au, pear, tet, elect, aguilarite, arsen, naumannite	siderite qtz, cal, dol, chl, marc, py, nontronite	1) Fe, Zn, Pb, Cu 2) Ag, Sb, Cu, Se	

Table 5. Volcanic rock-hosted silver deposits.

() Indicates reference

See abbreviation key p. 104

DISTRICT	VOLCANIC ROCKS	ORE CONTROL	MAJOR ALTERATION	MINERALIZATION	GANGUE	PARAGENESIS	SUPERGENE MINERALS
Hauraki, New Zealand (43)	andesite	fissures o.s.f. rep.	Silicification Argillic (Kaol-Qtz) (Ill-Mont) Prop (chl,cal,carb,py,ser)	pyra,cp,sp,gn,tet, elect,prou,poly, pear,naum,aguila- rite,cera,stib, argyrodite	qtz,py,marc, arsen	1) py,marc 2) b-metal,Ag min stib 3) cera 4) kaol	native Ag, hematite
Jarbidge, Nevada (47)	rhyolite	faults fissures	Silicification Sericite py,adularia	native Au,elect, arg,cera,naum,cp, pyra	qtz,ad,Si, apatite,bar, cal,chal, chl,ep,flu, py,hem,marc, clays		py and arg disappear
Milluach- aqui, Peru (25)	andesite	faults o.s.f.	Argillization (py) Prop (chl,ep,cal)	pyra,poly,acan,tet, gn,cp,sp	qtz,bar,cal, rhodc,gyp, flu,py,marc, arsen	1) py,marc 2) sp 3) gn 4) tet	native Ag, cerargyrite
Pachuca, Mexico (7)	andesite rhyolite dacite	fractures rep. o.s.f. (64)	Silicification Sericitization Prop (chl,carb,ep)	arg,sp,gn,cp,poly, steph	rhodonite, flu,qtz,py, bar,cal,dol	1) py,sp,qtz 2) gn,cp,arg 3) poly,steph,cal 4) rhodc 5) flu	native Ag, cov,chal, anglesite, arg
Tonopah, Nevada (55)	andesite dacite rhyolite- w/Sil. only	fractures rep. w/o.s.f.	Silicification - sericite, adularia,py,siderite,kaol, ep,chl,hem,cal	poly,arg,cera,gn, sp,Au,pyra,elect	qtz,py,ad, ser,carb	1) qtz,sp 2) gn,cp,pyra,arg, poly,carb,elect 3) gn,sp,qtz,poly, arg,cp,carb, elect (8)	cera,arg, native Ag, pyra,gyp,Si, malachite, Ag haloids (8)
Telluride, Colorado (27)	andesite rhyolite= poor ore (42)	fissures o.s.f.	ser,qtz,py,cal Prop (chl,ep,cal,py)	tet,ten,prou,sp, pear,arg,gn,cp, poly,pyra,Au (27,6)	qtz,py,cal, rhodc,anker- ite	1) qtz 2) py,arsen, rhodc 3) cp 4) sp 5) gn 6) tet,cp,poly 7) Au,carb	prou,arg, gyp,poly, pyra,native Ag,native Cu,chalco- cite
Summitville, Colorado (57)	rhyolite dacite latite	o.s.f.	Qtz-Alun (py,rut,leux) Ill-Kaol (qtz,rut,leux) Mont-Chl (ser,rut,jar,py, carb)	en,gn,sp,Au,Ag,Cu	py,bar, native S	Alteration pre- ceded mineraliza- tion	jar,kaol, Au,cov,MnO, limonite

Table 5 (cont.). Volcanic rock-hosted silver deposits.

() Indicates reference

See abbreviation key p.104

open-space filling and replacement occurs. At the Flathead mine, open-space fill textures are common in mineralized veins and indicate that fractures existed.

Extensive alteration typifies these epithermal type deposits. Silicification and propylitic alteration are ubiquitous within the volcanic rocks. Alunite occurs often in the most intensely silicified zone, most closely associated with ore deposition. Propylitic alteration (chlorite-carbonate-epidote) represents the least intense alteration, is transitional to fresh rock, and is generally the most widespread. Sandwiched between intensely silicified and propylitized zones is either a sericitized or argillized zone. The clay zones are also consistently zoned with dickite nearest the vein followed by kaolinite, illite, halloysite and montmorillonite progressively outward. Pyrite, jarosite, leucoxene, hematite and rutile commonly accompany the alteration types mentioned above; they have no spatial pattern. Adularia and zeolitic alteration are more rare.

Silicification is pervasive at the Flathead mine and alunite is closely associated with mineralization. Conditions at this deposit were favorable for argillic rather than sericitic alteration, though mixed-layer illite/smectites are potassic alteration products and may represent a lower temperature sericitic type zone. Kaolinite occurs closer to mineralization than the expansible-clays. Most of

the common alteration minerals of well-studied volcanic epithermal deposits exist at the Flathead mine.

The Flathead mine differs significantly from other volcanic rock-hosted silver deposits in that no propylitic alteration zone is apparent. Possible explanations for its absence are: 1) no surface expression is found due to post-alteration flows that cover the area; drill core is limited to the more intensely altered areas; 2) the hydrothermal front of the Flathead mine overlapped the hydrothermal fronts of nearby deposits (West Flathead, Ole, and Mary Ann mines) (fig. 1) effectively erasing the weak alteration zone; 3) the altering solutions remained strongly acidic beyond the limits of the volcanic host and were dissipated as brines at the surface (a very shallow deposit) and passed into Belt rocks laterally; 4) the Flathead mine represents an ancient hot-springs environment, and propylitic alteration occurs at much deeper levels, shallow level solutions being too acidic due to oxidation of H_2S , as in the geothermal fields of Iceland (Sigvaldason, 1963); and 5) it was eroded away prior to the deposition of the "sodic"-rhyodacite. The Flathead mine probably is a hot-springs deposit; explanations (3) and (4) appear most suitable.

The silver occurs in many minerals in epithermal deposits. Sulfides (argentite, acanthite, and stromeyerite) are commonly the primary silver minerals. Argentiferous galena is also common. Sulfantimonides (pyrargyrite,

polybasite, stephanite, and tetrahedrite), sulfarsenides (proustite, pearceite, and tennanite), selenides, tellurides and other silver sulfosalts are common. Common associated non-silver-bearing minerals include gold, sphalerite, galena, chalcopyrite and enargite. The mineralization within the volcanic rocks is commonly zoned with the silver content decreasing with depth (Sillitoe, 1977).

Silver occurs in galena in the low-grade ore at the Flathead mine. Shenon and Taylor (1936) recognized argentite and antimonial matildite (silver-bismuth-sulfide) in the high-grade ores. All of the non-silver-bearing minerals mentioned above also exist at the Flathead mine.

Typical gangue minerals of epithermal deposits besides the alteration products already noted include barite, marcasite, gypsum, fluorite and arsenopyrite. Barite is common in all areas of the Flathead mine. Marcasite is found at the dumps indicating its affinity with the high-grade ores.

Mineral paragenesis is highly variable in epithermal deposits but some generalities are apparent. Quartz and pyrite are always early but may have a second (later) period of formation. Gold is usually last to form. Silver precipitates late, either prior to or contemporaneous with gold. Galena is always later than sphalerite (see table 5). Evidence from the Flathead mine supports the early formation of pyrite. Galena is later than sphalerite but also has an earlier period of formation.

Supergene enrichment of silver occurs commonly in epithermal deposits, though it generally accounts for less silver than primary mineralization. Solutions must be acidic to dissolve silver from hypogene minerals and require sulfate for transport (Hurst, 1922). Shenon and Taylor (1936) report extensive secondary silver enrichment at the Flathead mine. Sulfates are present, as is oxidized pyrite, which could be the source of both SO_4 and acidic waters (Ransome, 1909).

The Flathead mine resembles other volcanic silver deposits in age, structural controls, ore and gangue minerals, ore textures and alteration. Its only significant difference is the apparent absence of the propylitic zone of alteration.

The Flathead mine most closely resembles the deposits at Goldfield, Nevada and Summitville, Colorado (table 5). The type of alteration most closely associated with ore mineralization at these deposits is silicification and aluniteization. Argillic alteration occurs farther from mineralization centers and kaolinite is a more advanced alteration product than is smectite. At these deposits, alteration preceded mineralization and provided space for ore deposition. However, the kaolinite facies at the Flathead mine probably originated after ore mineralization, similar to the formation of the advanced argillic assemblage at Hauraki, New Zealand (Ramsay and Kobe, 1974). Mixed-layer illite/smectites exist at Goldfield (Harvey and Vitaliano, 1964)

and the Flathead mine. Little ore extends into the argillic zone at Goldfield (Ransome, 1909) or at the Flathead mine.

The principal means of ore precipitation at these deposits is open-space filling. Leached phenocryst voids serve as sites for deposition (Goldfield - Ransome, 1909; Summitville - Steven and Ratté, 1960). The ore minerals at the Flathead mine more closely resemble those at Summitville (table 5).

CHAPTER VIII
SUMMARY AND CONCLUSIONS

Probable subduction related Tertiary volcanism produced the volcanic rocks and ore deposits of the Hog Heaven mining district. The Flathead mine alteration and mineralization apparently originated in the immediate vicinity of a volcanic vent (fig. 17) during the waning stage of the vent's volcanic activity.

A highly altered "potassic"-rhyodacite porphyry, formerly with a high sanidine phenocryst content, hosts the ore body at the Flathead mine. These rocks are predominantly extrusive as indicated by interbedded rhyolite and rhyodacite tuffs. The "potassic"-rhyodacite is intrusive at deeper levels.

The local drainage was apparently dammed by lava and/or ash flows because thin tuff units with fining-upward sequences, suggesting "quiet" water deposition, are common.

Some porphyry and tuff units contain numerous lithic fragments. Well-rounded Belt clasts imply either a period of stream reworking prior to incorporation in the flow or movement in a volcanic vent (i.e., breccia pipe).

After extrusion of these rocks a pervasive fracture

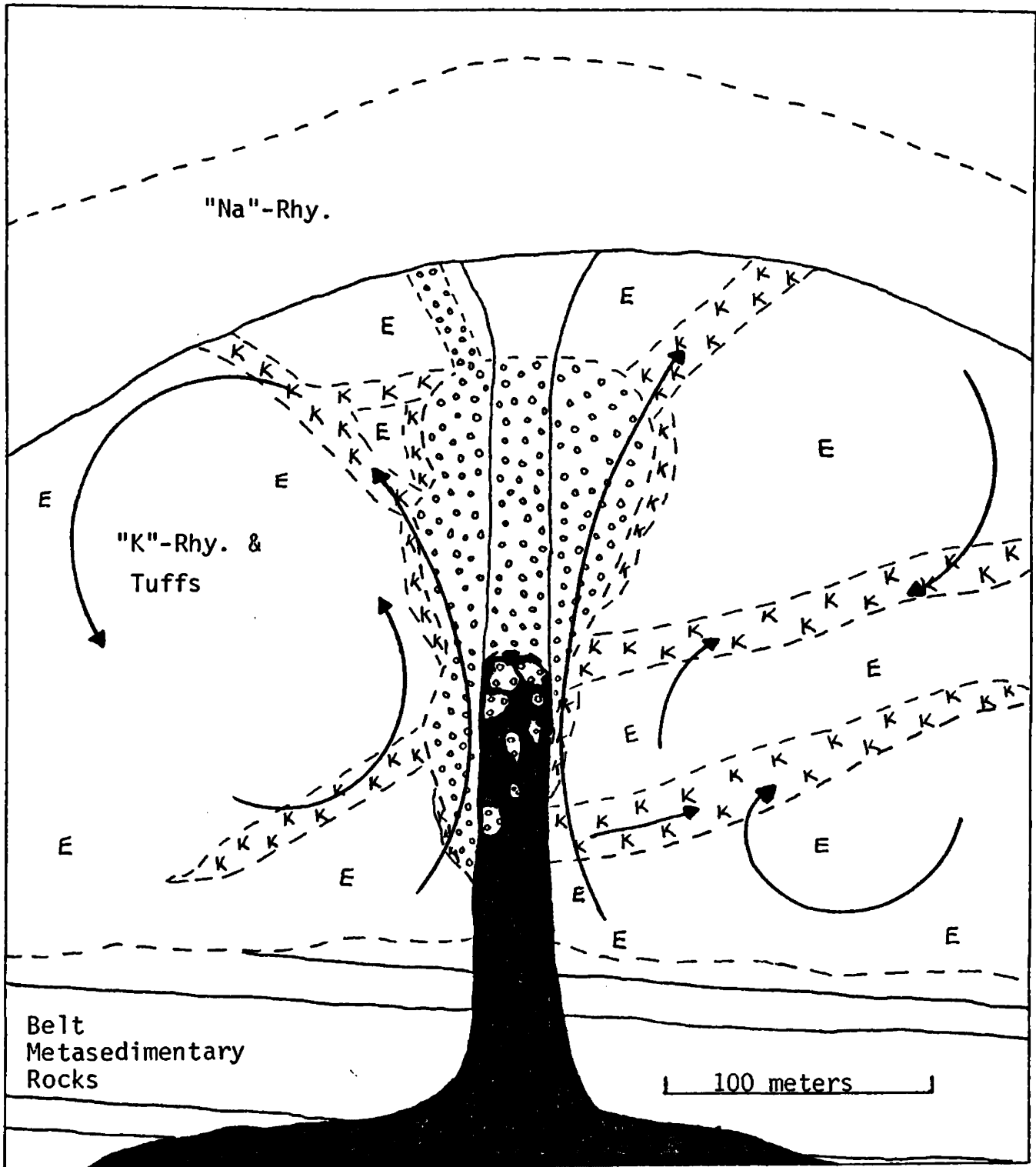


Fig. 17. Genetic model for the Flathead mine consisting of a hydrothermal convective cell in the area of a volcanic vent. The silicified core (••) and expansible-clay facies (E) formed early. The kaolinite facies (K) formed later as a result of mineralization and permeability (fracture) controls. The "sodic"-rhyodacite ("Na"-Rhy.) capped the area after cessation of the hydrothermal system.

system developed due, at least in part, to faulting. A hydrothermal convective cell of recirculated water (i.e., hot-springs) (fig. 17) developed, characteristic of the end stage of volcanism (Smith and Bailey, 1968). The water in such systems is generally meteoric (Sillitoe, 1977). The fractures served as avenues of transport for the hydrothermal solutions. Rock porosity independent of fracturing contributed to the circulation of solutions. This resulted in the formation of disseminated pyrite. Heat for mobilization of the hydrothermal fluids was provided by the underlying hypabyssal rocks.

The hydrothermal solutions were acidic and caused extensive wall-rock alteration. Cation exchange and leaching by hydrogen metasomatism were the dominant processes of the hydrothermal fluids in wall-rock alteration. In order of increasing hydrothermal stability, the primary minerals of the rhyodacites and rhyolites are: 1) amphibole (kaersutite); 2) biotite and sphene; 3) plagioclase (andesine); 4) sanidine and apatite; and 5) zircon.

The acidity of hydrothermal solutions circulating through the rock is buffered by wall-rock interactions during hydrogen metasomatism. Moderately acidic hydrothermal solutions were responsible for the development of an expansible-clay alteration assemblage. The distinguishing minerals of the expansible-clay facies (fig. 17) are smectite, randomly interstratified illite/smectite, rectorite,

and fresh primary sanidine. Pyrite also occurs here. Sanidine breaks down gradually in this facies.

The buffering capacity of the rocks is gradually exhausted as interactions with acidic solutions continue. Solutions, therefore, become more acidic. Maximum interaction between wall-rocks and hydrothermal solutions occurred where fracturing and rock porosity were greatest. This area is represented by the high-grade cellular ore (largely mined out) described by Shenon and Taylor (1936). The intense alteration here resulted in a zone (the core) (fig. 17) of extreme silicification with alunite. These rocks apparently developed numerous voids (i.e., phenocryst molds) due to the intense acid leaching. Abundant barite precipitated. The sulfuric acid necessary for the formation of sulfates originated by near-surface oxidation of H_2S and pyrite.

The numerous voids of the silicified core provided openings for mineral deposition as the ore-bearing solutions were introduced. Mineralization within the argillized fringe is less widespread, localized primarily in fractures.

Ore precipitation probably resulted largely from the mixing of meteoric water with metal-bearing solutions within the convective hydrothermal cell. This decreases the concentration of the complexing ion in the transporting complex and reduces the temperature resulting in decreased metal solubility. The association of ore minerals with sulfate minerals (barite and alunite) may not be entirely coinci-

dental. The reactions of sulfates with metal-transporting complexes may assist in sulfide precipitation either by oxidation or sulfate reduction depending on the type of metal-transporting complex. The argillized rocks (except where fractured) may have confined the ore-bearing solutions to the silicified core since argillization may reduce permeability (Park and MacDiarmid, 1975, p. 138). This would have led to enriched mineralization there.

Mineralization along fractures in the low-grade fringe was dominantly by open-space filling as indicated by crustification textures. Open spaces indicate shallow-depth environments. Some replacement also occurred in the low-grade fringe. Disseminated mineralization is less common. Pyrite and barite deposition generally preceded sphalerite and galena deposition. The galena is probably argentiferous as the silver content of the rocks is sympathetic to lead contents. Trace amounts of chalcopyrite are found.

A more advanced argillic alteration (kaolinite facies) (fig. 17) occurs where ore mineralization exceeds trace amounts. The precipitation of sulfides locally created more acidic hydrothermal solutions due to the release of H^+ from HS^- or H_2S . This caused more extensive leaching of silicate mineral cations. An abrupt front exists between the kaolinite and expansible-clay facies marked by the complete destruction of sanidine. At the kaolinite front, sanidine was no longer available to supply K^+ ions to stabilize

randomly interstratified illite/smectite and rectorite. Further leaching of Na^+ , Ca^{+2} , Mg^{+2} , and Si^{+4} destabilized smectite and K-clays. The remaining clay mineral is b-axis disordered kaolinite.

Quartz is present in both argillic facies either as a product of glass devitrification or silicification. Kaolinite exists in the expansible-clay facies also. The kaolinite-quartz assemblage suggests temperatures of formation below 400° C. The occurrence of mixed-layer illite/smectites with altered sanidine may indicate that temperatures never exceeded 200° C.

"Sodic"-rhyodacite lava(?) flows (fig. 17) originating from a different vent subsequently covered the earlier volcanic rocks and mineral deposits at the Flathead mine. Sanidine is much less plentiful relative to plagioclase in these rocks. These rocks subsequently underwent slight alteration, probably due to weathering.

Prospecting Suggestions

No large-scale symmetric zonation defines the alteration "package" at the Flathead mine. A silicified core is surrounded by different argillic alteration assemblages. This was due to variable rock permeability, largely controlled by fracturing.

Alteration is a good guide to mineralization at the Flathead mine because alteration accompanies mineralization, is more conspicuous than mineralization, and the richest ore

occurs in the most intensely altered rocks. However, the lack of symmetric zonation in the argillized fringe makes ore exploration more difficult. Detailed clay analysis is unnecessary as an exploration tool since the presence or absence of sanidine controls the type of argillic alteration that occurs and sanidine is commonly macroscopic. Extremely silicified rocks do not contain any clay.

Because post-mineralization flows cover the vicinity, alteration will be hidden from surface view. Chemical analyses of nonmineralized rocks may show anomalous metal values over buried hydrothermal systems due to secondary dispersion (p. 49). Possible target areas may be delineated by considering the deposits of the Hog Heaven mining district to be the outline of a volcanic crater or collapsed caldera. Craters (calderas) provide favorable plumbing systems for ore deposits (Smith and Bailey, 1968). The crater (caldera) outline could be projected as the continuation of the arc defined by the Ole, West Flathead, and Flathead or Mary Ann mines (fig. 1, p. 5).

BIBLIOGRAPHY

1. Alt, D.D., and Hyndman, D.W., 1978, Roadside Geology of Oregon: Mountain Press, Missoula, Mt., 268 p.
2. Aoki, K., 1963, The kaersutites and oxykaersutites from alkalic rocks of Japan and surrounding areas: Jour. Petrol., v. 4, part 2, p. 198-210.
3. Barnes, H.L., 1979, Solubilities of ore minerals, in Barnes, H.L.(ed.), Geochemistry of Hydrothermal Ore Deposits, 2nd Ed.: John Wiley, New York, p. 404-460.
4. _____, and Czamanske, G.K., 1967, Solubilities and transport of ore minerals, in Barnes, H.L.(ed.), Geochemistry of Hydrothermal Ore Deposits: Holt, Rinehart, and Winston, New York, p. 166-235.
5. Bastin, E.S., 1922a, Bonanza ores at the Comstock Lode, Virginia City, Nevada: U.S. Geol. Survey Bull. 735, p. 41-63.
6. _____, 1922b, Silver enrichment in the San Juan Mountains, Colorado: U.S. Geol. Survey Bull. 735, p. 65-129.
7. _____, 1948, Mineral relationships in the ores of Pachuca and Real Del Monte, Hidalgo, Mexico: Econ. Geol., v. 43, p. 53-65.
8. _____, and Laney, F.B., 1918, The genesis of the ores at Tonopah, Nevada: U.S. Geol. Survey Prof. Paper 104, 50 p.
9. Brindly, G.W., and Robinson, K., 1948, Structure of metahalloysite: Miner. Mag., v. 28, p. 393-406.
10. Bundy, W.M., 1958, Wall-rock alteration in the Cochiti mining district, New Mexico: New Mexico Bur. Mines and Min. Resources Bull. 59, p. 1-71.
11. Burbank, W.S., 1932, Geology and ore deposits of the Bonanza mining district, Colorado: U.S. Geol. Survey Prof. Paper 169, 166 p.

12. Coats, R., 1940, Propylitization and related types of alteration on the Comstock Lode: *Econ. Geol.*, v. 35, p. 1-16.
13. Coney, P.J., and Reynolds, S.J., 1977, Cordilleran Benioff zones: *Nature*, v. 20, p. 403-406.
14. Deer, W.A., Howie, R.A., and Zussman, J., 1966, *An Introduction to the Rock Forming Minerals*: Longman, London, 528 p.
15. Eberl, D., 1978, Reaction series for dioctahedral smectites: *Clays and Clay Mins.*, v. 26, p. 327-340.
16. _____, and Hower, J., 1975, Kaolinite synthesis: the role of the Si/Al and (alkali)/(H⁺) ratio in hydrothermal systems: *Clays and Clay Mins.*, v. 23, p. 301-309.
17. Farrah, H., Hatton, D., and Pickering, W.F., 1980, The affinity of metal ions for clay surfaces: *Chem. Geol.*, v. 28, p. 55-68.
18. Gianella, V.P., 1936, Geology of the Silver City district and the southern portion of the Comstock Lode, Nevada: *Univ. Nev. Bull.*, v. 30, no. 9, 108 p.
19. Goldich, S.S., 1938, A study in rock weathering: *Jour. Geol.*, v. 46, p. 17-58.
20. Gross, W.H., 1975, New ore discovery and source of silver-gold veins, Guanajuato, Mexico: *Econ. Geol.*, v. 70, p. 1175-1189.
21. Harrison, J.E., Griggs, A.B., and Wells, J.D., 1974, Preliminary geologic map of part of the Wallace 1: 250,000 sheet, Idaho-Montana: U.S.G.S. Open File Report, OF-74-37.
22. Harvey, R.D., and Vitaliano, C.J., 1964, Wall-rock alteration in the Goldfield district, Nevada: *Jour. Geol.*, v. 72, p. 564-579.
23. Heinrich, E. Wm., 1965, *Microscopic Identification of Minerals*: McGraw-Hill, New York, 414 p.
24. Hemley, J.J., and Jones, W.R., 1964, Chemical aspects of hydrothermal alteration with emphasis on hydrogen metasomatism: *Econ. Geol.*, v. 59, p. 538-569.
25. Hollister, V.F., and Entwistle, L.P., 1977, The Milluachaqui epithermal silver district of northern Peru: *Miner. Depos.*, v. 12, p. 235-238.

26. Hower, J., Eslinger, E.V., Hower, M.E., and Perry, E.A., 1976, Mechanism of burial metamorphism of argillaceous sediment: 1. Mineralogical and chemical evidence: Geol. Soc. America Bull., v. 87, p. 725-737.
27. Hurst, M.E., 1922, Rock-alteration and ore deposition at Telluride, Colorado: Econ. Geol., v. 17, p. 675-702.
28. Hyndman, D.W., 1972, Petrology of Igneous and Metamorphic Rocks: McGraw-Hill, New York, 533 p.
29. Johns, W.M., Smith, A.G., Barnes, W.C., and Page, W.D., 1963, Progress report on geologic investigations in the Kootenai-Flathead areas, northwest Montana: Montana Bur. Mines and Geol. Bull. 36, 68 p.
30. Joint Committee on Powder Diffraction Standards, 1980, Mineral Powder Diffraction File - Minerals: JCPDS, Swarthmore, Pa., 1168 p.
31. Krauskopf, K.B., 1979, Introduction to Geochemistry, 2nd Ed.: McGraw-Hill, New York, 617 p.
32. Krohn, D.H., and Weist, M.M., 1977, Principal information on Montana mines: Montana Bur. Mines and Geol., Sp. Pub. 75, 150 p.
33. Le Maitre, R.W., 1976, The chemical variability of some common igneous rocks: Jour. Pet., v. 17, p. 589-637.
34. Levinson, A.A., 1974, Introduction to Exploration Geochemistry: Applied Pub., Calgary, 612 p.
35. Lovering, T.S., 1950, The geochemistry of argillic and related types of rock alteration: Colo. Sch. Mines Quart., v. 45, p. 231-260.
36. Meyer, C., and Hemley, J.J., 1967, Wall-rock alteration, in Barnes, H.L.(ed.), Geochemistry of Hydrothermal Ore Deposits: Holt, Rinehart, and Winston, New York, p. 166-235.
37. Muffler, L.J.P., and White, D.E., 1969, Active metamorphism of upper Cenozoic sediments in the Salton Sea geothermal field and the Salton trough, southeastern California: Geol. Soc. America Bull., v. 80, p. 157-182.
38. Palache, C., Berman, H., and Frondel, C., 1951, Dana's System of Mineralogy, 7th Ed., V. II: John Wiley and Sons, New York, 1124 p.

39. Park, C.F., and MacDiarmid, R.A., 1975, Ore Deposits: W.H. Freeman, San Francisco, 529 p.
40. Petruck, W., and Owens, D., 1974, Some mineralogic characteristics of the silver deposits in the Guanajuato mining district, Mexico: Econ. Geol., v. 69, p. 1078-1085.
41. von Platen, H., 1965, Kristallisation granitischer Schmelzen: Contr. Min. Pet., v. 11, p. 334-381.
42. Purington, C.W., 1906, Ore-horizons in the veins of the San Juan Mountains, Colorado: Econ. Geol., v. 1, p. 129-133.
43. Ramsay, W.R.H., and Kobe, H.W., 1974, Great Barrier Island silver-gold deposits, Hauraki, New Zealand: Miner. Depos., v. 9, p. 143-153.
44. Ransome, F.L., 1909, The geology and ore deposits of Goldfield, Nevada: U.S. Geol. Survey Prof. Paper 66, 258 p.
45. Reynolds, R.C., and Hower, J., 1970, The nature of interlayering in mixed-layer illite-montmorillonites: Clays and Clay Mins., v. 18, p. 25-36.
46. Ross, S., and Smith, R.L., 1961, Ash-flow tuffs: their origin, geologic relations, and identification: U.S. Geol. Survey Prof. Paper 366, 81 p.
47. Schraeder, F.C., 1923, The Jarbidge mining district, Nevada: U.S. Geol. Survey Bull. 741, 86 p.
48. Schwartz, G.M., 1955, Hydrothermal alteration as a guide to ore: Econ. Geol., 50th Anniv. Vol., p. 300-323.
49. Shenon, P.J., and Taylor, A.V., 1936, Geology and ore occurrence of the Hog Heaven mining district, Flathead County, Montana: Montana Bur. Mines and Geol., Mem. 17, 26 p.
50. Sigvaldason, G.E., 1963, Epidote and related minerals in two deep geothermal drillholes, Reykjavik and Hveragerdi, Iceland: U.S. Geol. Survey Prof. Paper 450-E, p. 77-79.
51. Sillitoe, R.H., 1977, Metallic mineralization affiliated to subaerial volcanism: a review, in (anonymous), Volcanic Processes in Ore Genesis: Geol. Soc. London, Sp. Pub. 7.

52. Skoog, D.A., and West, D.M., 1980, Principles of Instrumental Analysis, 2nd Ed.: Saunders College, Philadelphia, 769 p.
53. Smith, R.L., and Bailey, R.A., 1968, Resurgent cauldrons: Geol. Soc. America Mem. 116, p. 613-662.
54. Sparks, R.S.J., Self, S., and Walker, G.P.L., 1973, Products of ignimbrite eruptions: Geology, v. 1, no. 3, p. 115-118.
55. Spurr, J.E., 1905, Geology of the Tonopah mining district, Nevada: U.S. Geol. Sur. Prof. Pap. 42, 295 p.
56. Šrodón, J., 1980, Precise identification of illite/smectite interstratifications by x-ray powder diffraction: Clays and Clay Mins., v. 28, p. 401-411.
57. Steven, T.A., and Ratté, J.C., 1960, Geology and ore deposits of the Summitville district, San Juan Mountains, Colorado: U.S. Geol. Survey Prof. Paper 343, 70 p.
58. Stout, G.H., and Jensen, L.H., 1968, X-ray Structure Determination: MacMillan, New York, 467 p.
59. Tolman, C.F., and Ambrose, J.W., 1934, The rich ores of Goldfield, Nevada: Econ. Geol., v. 29, p. 255-279.
60. Urabe, T., 1978, Quartz simultaneously precipitated with Kuroko ores in the Uwamuki No. 4 deposit, Kosaka mine: Mining Geol., v. 28, p. 337-348.
61. Vance, J.A., 1969, On synneusis: Contrib. Min. Petrol., v. 24, p. 7-29.
62. White, D.E., 1955, Thermal springs and epithermal ore deposits: Econ. Geol., 50th Anniv. Vol., p. 99-154.
63. Williams, H., Turner, F.J., and Gilbert, C.M., 1954, Petrography: W.H. Freeman, San Francisco, 406 p.
64. Wisser, E., 1951, Tectonic analysis of a mining district: Pachuca, Mexico: Econ. Geol., v. 46, p. 459-477.

APPENDIX

<u>Vertical Holes ;</u> Sample # : Depth		<u>Angle-Holes ; Sample #</u> : Vertical Depth ; (Down-hole Depth)		
<u>H-17</u>	<u>H-4</u>	<u>H-20</u>	<u>H-2</u>	<u>H-6</u>
1: 18'	1: 14'	1: 10.3' (14.5')	1: 15.6' (18')	1: 12.7' (14')
2: 49.2'	2: 25.7'	2: 33.9' (48')	2: 43.3' (50')	2: 46.2' (51')
3: 77'	3: 51.3'	3: 52.3' (74')	3: 58' (67')	3: 64.8' (71.5')
4: 82.4'	4: 92.2'	4: 78' (110.4')	4: 91.4' (105.5')	4: 82.5' (91')
5: 112'	5: 98'	5: 150.6' (213')	5: 118.6' (137')	5: 92.4' (102')
6: 169'	6: 112'	6: 176' (249')	6: 161' (186')	6: 112.4' (124')
7: 176'	7: 144'	7: 244' (345')	7: 220' (254')	7: 142.3' (157')
8: 178'	8: 206'	8: 258' (365')	8: 239' (276')	8: 155' (171')
9: 187.5'	9: 224'	9: 344.3' (487')	9: 281.5' (325')	9: 186.2' (205.5')
10: 191'	10: 263'	10: 391' (553')	10: 293.3' (338.7')	10: 192.1' (212')
11: 201'	11: 315'	11: 434.8' (615')	11: 324.8' (375')	11: 204.8' (226')
12: 232'	12: 376'	12: 448.3' (634')	12: 329.5' (380.5')	12: 213' (235')
13: 295'	13: 390'	13: 481.5' (681')	13: 370.1' (428')	13: 242.9' (268')
14: 319'	14: 480'		14: 415.7' (480')	14: 270' (298')
15: 322.4'	15: 527.5'		15: 430.4' (497')	15: 275.5' (304')
16: 370'	16: 540.5'		16: 494.9' (571.5')	16: 333.5' (368')
17: 387'	17: 568'		17: 553.8' (639.5')	17: 387.9' (428')
18: 398'	18: 574'		18: 584.6' (675')	18: 437.4' (482.6')
19: 414'	19: 610.8'		19: 618.9' (714.7')	19: 462.2' (510')
20: 437'	20: 621.1'		20: 679.8' (785')	20: 560.1' (618')
21: 484'	21: 639'			21: 622.6' (687')
22: 500.5'	22: 649'			
23: 540'				
24: 563'				
25: 596'				
26: 693'				

Appendix 1. Drill-core samples.

SAMPLE	H2-2	H2-9	H2-12	H2-17	H4-3	H4-4	H4-7
MINERALOGY							
Sanidine	15%; ≤1.5mm	15%; ≤5mm; Carlsbad tw.; broken; embayed	15%; ≤2.5mm	Hand sample	12%; ≤2.5mm; broken	5%; <1mm	7%; ≤2mm; broken
Plagioclase	15%; ≤1.5mm; Albite twins	<1%	2%; Albite twins		1%; ≤.5mm	tr.	
Accessory Prim. Mins.	tr. Zircon	Biotite, mostly alt'd	Apatite, to .75mm; tr. Zircon	Apatite		tr. Zircon	tr. Zircon
Fe Oxides + Hydroxides	Limonite, minor		Hematite, <1%	3% Limonite	25% Hematite, microveins; 15% Limonite	tr. Hematite	tr. Hematite
Leucoxene		1%; rep. ghost xtyls.		3%; rep. amphibole + borders; oriented		<1%	1% including Rutile
Additional Secondary Minerals		Sericite	Sericite rep. biotite	Carbonate 5%, rep. feld; tr. Sericite			tr. Sericite
Pyrite	1%	3% dissem- inated	3%	3%; conc. in stringers; dissem. in altered phenocrysts	tr.	4%	1%
Mineralization			1% Sphaler- ite rep. biot. cleav. 1% Barite			tr. Galena + Sphalerite	
Lithics							?, houses sericite
Groundmass & Alt. Phenos.	Qtz.	Qtz. + Rec- torite; Rect. confined to alt. phenos.	Clay and/or feld. + Qtz.	Rectorite, Kaolinite + Qtz.	Qtz., Mix- Layer clay + Kaolinite	Clay and/or feld. + Qtz.	Qtz. + clay and/or feld.

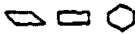
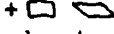
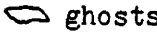
Appendix 2a. Mineralogy of "potassic"-rhyodacites (expansible-clay facies).

SAMPLE MINERALOGY	H4-8	H4-13	H4-15	H6-2	H6-6	H6-20	H6-21
Sanidine	25%; to 9mm; Carlsbad twins; broken	Carlsbad twin, 3.5mm	2%	6%; ≤2mm; broken	3%; ≤2mm	10%; ≤4mm ; Carlsbad twins; broken	10%; ≤3mm; broken
Plagioclase		12%; ≤3.5mm; Albite twins some altered borders; Glom- erocrysts				2%; ≤2mm; embayed	
Accessory Prim. Mins.		tr. Apatite		tr. Zircon			Qtz., broken; embayed
Fe Oxides + Hydroxides		1% Hematite	Limonite, minor	Limonite, moderate	tr. Hematite		
Leucoxene	1%; rep.  ghosts	1%; replaces amphibole,  ghosts	1%; rep. amphibole +  ghosts		rep. ghosts crystals	1%; rep.  ghost	1-2%; rep.    ghosts
Additional Secondary Minerals	tr. Sericite		Sericite, <1%, rep. biotite + amphibole				
Pyrite	2%; dissemi- nated	3%; veinlets cut feldspar; rep. skeleton crystals	4%; veinlets	4%; dissemi- nated		2%; veinlets	2%
Mineralization			tr. Barite	tr. Sphal- erite			Sphalerite?
Groundmass & Alt. Phenos.	Qtz. + clay feld?	Qtz. + clay feld?	Qtz., undulose	Clay, feld?, Qtz.	Qtz. + Smectite + Kaolinite	Clay, feld?, SiO ₂ mins.	Rectorite + Kaolinite

Appendix 2b. Mineralogy of "potassic"-rhyodacites (expansible-clay facies).

SAMPLE MINERALOGY	H17-13	H20-5	H20-8	H2-5	H2-6	H6-18	H17-5
Sanidine	9mm Carlsbad twin; Zoned	2%; ≤4mm	3%; ≤4mm; Carlsbad tw.	8%; ≤3mm	5%; ≤1mm	6%; ≤1mm	12%
Plagioclase	tr.			7%; ≤.8mm; Albite twins	10%; ≤1mm; Albite twins	tr. Albite twins	1%; Albite twins
Accessory Primary Minerals	Biotite, mostly alt'd	Apatite Zircon	Apatite Zircon Qtz. (prim?)	tr. Zircon tr. Biotite	tr. Biotite		tr. Zircon
Fe Oxides + Hydroxides				1% Hematite in vein w/ Limonite		Limonite	3% Limonite
Leucoxene	2%	1%; rep.  ghosts	1%			trace	
Add. Sec. Mins.		tr. Sericite	2% Carbonate rep. feld.	Sericite in lithics	Sericite in lithics	6% Carbonate Sericite	Sericite
Pyrite	3%	3%	5%, veins	trace	<1%	1%	
Mineralization		tr. Sphalerite	Sphalerite?		tr. Sphalerite		
Lithics				Yes	Yes	Yes	Yes
Groundmass & Alt. Phenos.	Kaolinite + Smectite + Qtz.	Qtz. (undulose) + Rectorite + Smectite	Rectorite + Qtz.	v. fine low-biref. mins.	Qtz. + clay and/or feld	Qtz. + clay and/or feld.	Qtz. + clay and/or feld

Appendix 2c. Mineralogy of "potassic"-rhyodacites (expansible-clay facies).

SAMPLE MINERALOGY	H2-18	H2-20	H4-9	H4-10	H4-16	H4-21	H6-1	H20-3	H20-11
Primary Minerals	trace Zircon	Qtz., embayed		tr. Zircon Qtz(prim?)		tr. Zircon Qtz(prim?)	tr. Magnetite		tr. Apatite
Fe Oxides + Hydroxides	tr. Hematite	Limonite surrounds pyrite	Hematite, 20%; Limonite, 48%				Hematite, 3% from magnetite; Limonite, 5%	Hematite, 10%; Goethite, 20%	
Leucoxene	1%; rep. 	trace	trace	1%; rep. amphibole +  ghosts	2%; rep. ghosts	<1%; rep.  ghosts	1%; rep. 	2%; rep.  ghosts	
Additional Secondary Minerals	Alunite?	1% Alunite	trace Sericite						6% Carbonate, veins + dissem. tr. Ser.
Pyrite	4%; disseminated	3%		5%; veins cut feld.; rep. mafics	12%	4%	<1%	2%, some veins	3%; vein + dissem.
Mineralization	Sphalerite 3%; Galena <1% Barite <1% rep.feld.	Sphal. 4% Galena <1%		tr. Sphal. tr. Galena	Sphalerite 2% Galena 1% Barite 4%	Sphalerite <1%		tr. Sphal. 1% Galena veins tr. Bar.	1% Sphal.
Groundmass & Alt. Phenos.	Qtz.	Kaol. + Qtz.	Qtz. + Kaol.	Qtz. + clay	Qtz., undulose	Kaol. + Qtz., undulose	Kaol. + Qtz.	Qtz. + clay	Qtz. undulose

Appendix 3a. Mineralogy of "potassic"-rhyodacites (kaolinite facies).

SAMPLE MINERALOGY	H2-19	H4-18	H4-19	H6-7	H6-9	H6-12	H6-15	H17-11	H17-21
Primary Minerals	Biotite, mostly altered	Zircon tr.	Zircon tr.	Zircon tr.		Zircon tr.	Zircon tr.	Zircon tr.	Zircon tr.
Fe Oxides + Hydroxides	Limonite, minor			Hematite, trace	Mag.+Hem. 3%; Goethite, 5%	Mag. tr. Hem. 3% Goethite, 6%	Limonite	Hematite, tr.	Hematite, 1%
Leucoxene	trace	trace	<1%	1%		<1%		1%; rep. ghosts	
Additional Secondary Minerals			Microlite high-bi-refs.	Sericite trace			Jarosite?		
Pyrite	10%	8%; veins	7%	5%; vein, dissem., alt.pheno edges	1%			2%	2%
Mineralization	tr. Galena + Sphalerite	8% Sphal. 2% Galena veins		<1% Sphal. <1% Gal. veins + dissem.	tr. Sph.			1% Galena 1% Sphal-erite	<1% Gal. 1% Sphal.
Groundmass & Alt. Phenos.	v. fine low-biref. mins.	Qtz.	Qtz. + clay	Qtz. + clay	Kaol. + Qtz.	Qtz. + clay	Qtz.	v. fine low-biref. mins.	Qtz. + Kaolinite
Lithics	w/pyrite	Yes	w/pyrite; rounded	Yes	Yes	Yes	Yes	Yes	w/ser.-muscovite

Appendix 3b. Mineralogy of "potassic"-rhyodacites (kaolinite facies).

SAMPLE	H6-14	H20-1
MINERALOGY		
Primary Mins.		trace Zircon
Fe Oxides + Hydroxides	4% Limonite	2% Hematite; 3% Limonite; veins
Leucoxene	trace	2%; rep. 
Additional Secondary Minerals	Tridymite, crustiform; high-biref. microlites	
Pyrite		1%
Mineralization	20% Barite, veins, olso- cherite	2% Barite, veins + pheno. casts
Groundmass & Alt. Phenos.	Quartz + microlites	Quartz

Appendix 4. Mineralogy of extremely silicified rocks.

SAMPLE MINERALOGY	H2-8	H17-1	H17-9	H17-10	H6-11	H17-14	H17-15	H17-23	WP-6
Sanidine	5%; ≤.8mm	2%; ≤2mm	30%; ≤.4mm	20%; ≤.8mm					
Plagioclase	3%; ≤.8mm; Albite twins	2%; ≤2mm; Albite twins	20%; ≤.3mm; Albite twins	7%; ≤.8mm; Albite twins					
Accessory Primary Minerals	Qtz. (prim?)		Quartz, 20%; ≈.3mm tr.Zircon	Quartz		2% Qtz, <1mm; tr.Zircon	Zircon		Zircon Qtz. (prim?)
Fe Oxides + Hydroxides					1% Magnet.	3% Hema- tite; Limonite			1% Hema- tite
Leucoxene						1% rep. ◊	3%		1%
Additional Secondary Minerals	Sericite mainly in lithics	tr. Ser- icite	tr. Ser- icite	Sericite in lithics		Alunite + Jarosite microlites 20%		Sericite, <1%	
Pyrite	<1%		1-2%, conc. in layers	<1%	10%, dissem. + stringers		3%, dissem.	3%, dissem. + conc. in layers	
Mineralization		2% Barite rep.plag.				4% Barite		2% Sphal- erite	
Lithics	Yes, rounded	Yes		Yes, rounded			Yes		Yes, rounded
Groundmass	v. fine low-biref. mins.	Qtz. + clay and/ or feld.	Qtz. + Kaolinite	v. fine low-biref mins.	Qtz. + Kaolinite	Qtz.	Qtz. + clay	Qtz. + kaol?	Qtz. + clay

Appendix 5. Mineralogy of rhyolite-rhyodacite tuffs.

SAMPLE MINERALOGY	H2-1	WP-7	YL-7	TA-C	FR	P-UP	P-F
Plagioclase	25%; <8mm; Albite twins Broken; Zoned; Glom- erocrysts	30%; ≤4mm; Albite, Per- icline, Carlsbad twins; Zoned; Glomerocr.	30%; ≤4.5mm; Albite twins Zoned; Glom- erocrysts	25%; ≤3.5mm; Albite twins Glomerocr.	30%; ≤4mm; Albite, Per- icline twins Zoned; Glom- erocrysts	40%; ≤7mm; Albite twins Zoned; Glom- erocrysts	30%; ≤3.5mm; Albite twins Zoned; Glom- erocrysts
Sanidine	1%; <2mm; enclosed by plag.	1% ≤2mm; Carlsbad twins	1%; plag. inclusions; enclosed by plag.	4%; ≤3mm	6%; ≤3.5mm; plag. inclu- sions	2%; ≤3mm	3%; ≤4mm
Accessory Primary Minerals	2% Biotite, some bent; <1% Sphene; tr. Apatite	2% Biotite; 2% Apatite; 1% Sphene, twinned	2% Biotite; tr. Sphene; tr. Zircon; tr. Apatite	2% Biotite; 1% Sphene ; tr. Magnet.	2% Biotite, ≤2.1mm; tr. Apatite	2% Biotite; tr. Zircon	2% Biotite; tr. Apatite
Fe Oxides + Hydroxides	2% Hematite; tr. Magnet. on sphene borders	2% Magnet.+ Hematite		1% Hematite rep. Mag.	1% Magnetite	1% Magnetite	tr. Magnet.
Leucoxene	tr. rep. sphene borders	rep. sphene	2% rep. sphene	tr. rep. sphene	1% rep. sphene + amphibole	1%	tr.
Add. Sec. Min.		tr. Muscovite rep. biotite					
Groundmass	Smectite + Qtz. (+feld?)	Smectite + Qtz. (+ feld?)	Clays + Qtz. (+ feld?)	v. fine low-biref. mins.	Smectite + Qtz. (+ feld?)	Smectite + Qtz. (+ feld?)	Smectite + Qtz. (+ feld?)

Appendix 6. Mineralogy of "sodic"-rhyodacites.

Table Abbreviations

acan = acanthite	kaol = kaolinite
allo = allophane	leux = leucoxene
alun = alunite	mag = magnetite
arg = argentite	marc = marcasite
arsen = arsenopyrite	mont = montmorillonite
bar = barite	naum = naumanite
bis = bismuthinite	o.s.f. = open-space fill
bn = bornite	pear = pearceite
cal = calcite	poly = polybasite
carb = carbonate	prou = proustite
cera = cerargyrite	py = pyrite
chal = chalcedony	pyra = pyrargyrite
chl = chlorite	qtz = quartz
clinoz = clinozoisite	rep. = replacement
cov = covellite	rhodc = rhodocrosite
cp = chalcopyrite	rut = rutile
elect = electrum	Sil. = silicification
en = enargite	Ser = sericitization
ep = epidote	smec = smectite
fam = famatinite	sp = sphalerite
gn = galena	steph = stephanite
gyp = gypsum	stib = stibnite
halloy = halloysite	strom = stromeyerite
hem = hematite	ten tennantite
ill = illite	tet = tetrahedrite
jar = jarosite	verm = vermiculite

Appendix 7. Abbreviations used in Tables.